2007-09-14

Principles, Functions, and Concepts for Compliant Mechanically Reactive Armor Elements

Cameron S. Andersen
Brigham Young University - Provo

PRINCIPLES, FUNCTIONS AND CONCEPTS FOR COMPLIANT

MECHANICALLY REACTIVE ARMOR ELEMENTS

by

Cameron S. Andersen

A thesis submitted to the faculty of

Brigham Young University

in partial fulfillment of the requirements for the degree of

Master of Science

Department of Mechanical Engineering

Brigham Young University

December 2007

BRIGHAM YOUNG UNIVERSITY

GRADUATE COMMITTEE APPROVAL

of a thesis submitted by

Cameron S. Andersen

This thesis has been read by each member of the following graduate committee and by majority vote has been found to be satisfactory.

_____	_____
Date	Spencer P. Magleby, Chair
_____	_____
Date	Larry L. Howell
_____	_____
Date	Brian D. Jensen

BRIGHAM YOUNG UNIVERSITY

As chair of the candidate's graduate committee, I have read the thesis of Cameron S. Andersen in its final form and have found that (1) its format, citations, and bibliographical style are consistent and acceptable and fulfill university and department style requirements; (2) its illustrative materials including figures, tables, and charts are in place; and (3) the final manuscript is satisfactory to the graduate committee and is ready for submission to the university library.

_____   _____
Date   Spencer P. Magleby
                                                               Chair, Graduate Committee

Accepted for the Department

                                                    _____
                                                               Matthew R. Jones
                                                               Graduate Coordinator

Accepted for the College

                                                    _____
                                                               Alan R. Parkinson
                                                               Dean, Ira A. Fulton College of
                                                               Engineering and Technology

ABSTRACT

PRINCIPLES, FUNCTIONS AND CONCEPTS FOR COMPLIANT

MECHANICALLY REACTIVE ARMOR ELEMENTS

Cameron S. Andersen

Department of Mechanical Engineering

Master of Science

There exists a great need for armor systems with greater mass efficiencies and ballistic limits. This thesis explores the development of a new field of armor capable of satisfying the increased demand for modern armor: Mechanically Reactive Armor or MRA. More specifically, the thesis focuses on Compliant MRA or CMRA.

From the physics governing projectile-armor interactions, principles governing successful design of MRA are identified and presented. These principles or design approaches focus primarily on rejecting, minimizing, or absorbing the incoming projectile's kinetic energy. After identifying these principles, the specific mechanical functions required by the principles are isolated. These functions represent the physical behavior and capabilities of real mechanisms that satisfy the specific design principles. Using these mechanical functions and other benchmark concepts as a guide, established concept generation methodology is used to identify families of CMRA concepts that could supply the identified mechanical functions. These concept families are then narrowed by comparison of their respective

ability to supply the required mechanical functions. The remaining concepts are selected for further study and simulation.

In order to provide more detailed insight into the behavior of specific designs of these concepts, a quantitative model is developed. This simplified model is capable of predicting the behavior of the CMRA system when impacted by a ballistic projectile. After development, the model is then implemented to search the design space of the narrowed concepts. The search of the design space reveals important trends to be used in the design of CMRA elements. Finally, the feasibility of the specific designs is evaluated to judge their practicality in terms of practical materials and dimensions. It is shown that the concepts hold significant promise but require further design and development to provide the most desirable performance.

ACKNOWLEDGMENTS

This thesis is in many ways the result of a collaboration of the effort of many individuals.

I would like to thank the Brigham Young University Compliant Mechanisms Research Group for countless hours of assistance as a sounding board for my research. Many of the challenging aspects of my research were made much easier with their help. Additionally, I offer my heartfelt gratitude to the Ira A. Fulton College of Engineering and Technology for the financial support of this work.

I would also like to extend my special thanks to my graduate advisor, Dr. Spencer Magleby, for his invaluable counsel and advice at every stage of this research. His guidance has consistently improved my efforts and inspired my mind. Further thanks are also due to Dr. Larry Howell and Dr. Brian Jensen, who also sit on my graduate committee. Their professional input has provided perspective that has always been profitable.

I wish to thank my wife Kelli for her unending love and support. The long hours necessary for completion of a thesis were truly a mutual investment, and I appreciate her willingness to give up so much in this effort. She is and always will be my best inspiration.

Finally, I wish to thank my Father in Heaven for the aid and support that always came when it was most needed, and for sending such a consistent stream of ideas, hope, and peace into my life.

Table of Contents

List of Tables

List of Figures

Chapter 1

Introduction

1.1 Motivation

Operation Iraqi Freedom, launched by United States and United Kingdom forces against Iraq on March 19, 2003, has been the latest of a series of modern conflicts involving the use of Armored Fighting Vehicles (AFVs). The most common AFVs engaged in combat today range from the HMMWV (High-Mobility Multipurpose Wheeled Vehicle or "Humvee") on the light end to the M1-A1 Abrams tank on the heavy end. These AFVs are arrayed with a wide variety of armor systems, many of which are either inadequate to meet likely threats or excessively massive.

The M998 Humvee (Figure 1.1), which is the most commonly deployed tactical vehicle by the United States Armed Forces [1], is particularly vulnerable to attack because it was not originally intended to be used as an AFV and bears little or no armor as manufactured. After the addition of extra armor plating to under-armored Humvees, these "Up-Armored Humvees" are much more likely to break down or roll over due to the extra mass and elevated center of gravity. It is estimated that as of April 15, 2006, perhaps one in four American lives spent in Iraq could have been spared if all combat-engaged Humvees had been armored adequately [2].

As demonstrated by the post-production armoring of Humvees, attempts to increase an armor system's ability to stop kinetic energy weapons, or "stopping power", has traditionally required a costly increase in the mass of the system. The literature [3, 4] documents a variety of strategies for improving armor system efficiency, the stopping power to mass ratio, as compared with traditional approaches. These lightweight armor systems often include ceramic or composite matrices, unique structural alignment (layering, spacing, etc.),

Figure 1.1: M998 HMMWV or "Humvee"

or reactive elements. While these new systems are often quite successful, many implementations are impractical because they are overly expensive and complicated.

Mechanically Reactive Armor (MRA) is here defined to be a specialized subset of reactive armor systems. MRA systems is designed to minimize a kinetic energy projectile's penetration power by using a kinematic mechanism or linkage to effectively deflect and/or absorb its kinetic energy. In many cases, this is accomplished by harnessing the projectile's momentum and kinetic energy and transforming it with the motion of the mechanism or linkage.

Compliant Mechanically Reactive Armor (CMRA) is a subset of MRA where the armor mechanism or linkage is compliant. Compliant mechanisms offer great advantages to the functions and production of MRA, as will be discussed later. The conceptual nature of much of this research is such that the principles, functions, and concepts developed apply both to rigid-body and compliant MRA systems. This research is pursued from the perspective that compliant mechanism technology renders feasible many of the MRA concepts that might otherwise be impractical in rigid-body form. However, because the various discussions to follow apply to both MRA and CMRA, the terms may be used interchangeably under the assumption that CMRA will generally offer refined versions of any MRA design. The advantages of compliant mechanism technology are specifically addressed in Chapter 2.

1.2 Objective

It is the objective of this research to investigate this new field of armor. Specifically, this involves the identification of the governing design principles of MRA systems and the isolation of the mechanical functions required to satisfy these principles. The research will further entail the generation of specific innovative concepts that embody and satisfy these principles and functions using established design and development methodology. After their generation, these concepts will be evaluated qualitatively and narrowed using the design principles previously identified. A new impact simulation model will also be developed to provide a quantitative basis for searching the design space of the selected concepts. Finally, conclusions and recommendations founded on the results of these research steps will be drawn and presented.

1.3 Thesis Outline

The remainder of the thesis is organized to meet these objectives, and will be outlined as follows. Chapter 2 provides a review of the relevant literature, including patents and scholarly papers and texts. Chapter 3 outlines the methodology used to accomplish the objectives. Chapter 4 presents the principles identified as a guide for the design of CMRA elements. Chapter 5 draws from these principles the mechanical functions required by a successful CMRA element. Chapter 6 presents the concepts generated. Chapter 7 details the preliminary screening processes to narrow the concepts, and then lays a foundation for further quantitative concept evaluation. Chapter 8 outlines the development and validation of the quantitative model capable of simulating ballistic impact into the CMRA elements. Chapter 9 describes the application of the model to evaluate the narrowed concepts and search the design space. It also discusses the trends within the design space and identifies the desirable design goals. The practical feasibility of the desirable regions of the design space is also considered. Finally, Chapter 10 draws conclusions and makes recommendations for future research.

Chapter 2

Literature Review

2.1 Introduction

This chapter will present a review of the scholarly literature relevant to this thesis. First, a review of rigid-body and compliant mechanisms will be given, including their characteristic advantages and opportunities. Next, a brief review of impact mechanics and terminal ballistics will be presented. Finally, the current state of technology in the design of ballistic armor systems will be reviewed.

2.2 Rigid-Body and Compliant Mechanisms

A kinematic mechanism is a mechanical device that transfers or transforms energy, motion, or forces [5]. These mechanisms are commonly found in rigid-body form, being formed from multiple rigid links joined by movable joints. Such mechanisms are incredibly useful and versatile, and are employed in a wide variety of applications. Automobile engines employ rigid-body mechanisms to transfer the linear motion of pistons into rotational motion of the wheels. Self-locking pliers, as shown in Figure 2.1, employ a rigid-body mechanism to multiply the user's input gripping force many times to increase the plier's output gripping force.

A *compliant* mechanism may accomplish the same functionality of a rigid-body mechanism, but does so by the deflection of one or more flexible members [5]. These compliant mechanisms often replace pin joints and rigid beams with compliant segments. As these flexible members deflect, they store energy and exert forces internal to the mechanism, making possible several significant advantages. Among these advantages over traditional rigid-body mechanisms are the ability to construct a mechanism with unique force-deflection relationships, reduced part-count and wear, increased precision, reduced mass,

Figure 2.1: Self-locking pliers composed of a rigid-body force-multiplying mechanism

Figure 2.2: Compliant fishhook pliers [5]

and easier manufacturability. These advantages are of particular interest in the design of armor systems where mass, force-deflection relationships, and manufacturability are critical. A compliant counterpart of the rigid-body self-locking pliers shown in Figure 2.1, the crimping mechanism in Figure 2.2 [5] uses compliant joints and members to provide a similar function.

2.2.1 Pseudo-Rigid Body Model

The Pseudo-Rigid Body Model (PRBM) is a powerful approach used to simplify the complex large-deflection analysis of compliant mechanisms [5]. The PRBM replaces beams and joints with multiple rigid beams joined by torsional springs and pin joints at specific positions along the length of the original beam. This method preserves the behavior of the compliant beam but allows use of the much simpler analysis techniques for rigid-body mechanisms. The PRBM incorporates different loading and boundary conditions, as well as beam material and geometry properties into the simplified rigid-body model by controlling the spring constants and pin joint locations.

2.3 Impact Mechanics

A full review of the mechanics of impacts and collisions is beyond the scope of this thesis, but a brief review of the basic physics will be presented in order to better understand the concepts and modelling employed in this thesis.

2.3.1 Rigid-Body Collisions

For any type of collision without external impulses, the momentum of the entire system is conserved; that is, the momentum just before the collision equals the momentum just after the collision. When kinetic energy *and* momentum are conserved, the impact is called *perfectly elastic*. This represents the most simple type of collision and is shown in Figure 2.3. Here, mass particles *A* and *B* have initial velocities $v_{A,i}$ and $v_{B,i}$, respectively. During the impact, the particles compress elastically and then rebound with redistributed energy. The redistribution, which depends on the masses of the two particles, may result in rebound velocities in the same or differing directions, as shown in the figure. This redistribution is such that the velocity of the center of mass of the system and the relative velocity between the two particles remains constant before and after the impact. Alternatively, if $m_A = m_B$, the relative velocity of one particle with respect to the other is inverted by the impact:

$$v_{A,i} - v_{B,i} = v_{B,f} - v_{A,f} \qquad (2.1)$$

Kinetic energy, however, is usually not conserved during a collision because of its conversion to thermal or potential energy. A *perfectly inelastic* collision is one in which the particles remain conjoined after the impact and have a common final velocity. This is illustrated in Figure 2.4. As before, momentum is conserved, allowing the following momentum balance.

$$m_A v_{A,i} = (m_A + m_B) v_f \qquad (2.2)$$

7

(a) before collision   (b) after collision

Figure 2.3: Perfectly elastic collision of particles A and B both before and after collision

(a) before collision   (b) after collision

Figure 2.4: Perfectly inelastic collision of particles A and B both before and after collision

where m_A and m_B are the masses of the two particles, $v_{A,i}$ is the initial velocity of particle A and v_f is the common final velocity of the particles. This relationship allows prediction of post-impact behavior given the pre-impact states.

2.4   Terminal Ballistics

Terminal ballistics is a rapidly developing field of research addressing the reaction occurring between a ballistic projectile and a target. In this case, the collision occurs at relatively high velocities (100 to 1000 m/s), and the reaction and results are complex functions of target and projectile geometry and properties. The complexity stems largely from the nonlinear plastic energy dissipation and elastic energy storage which are crucial to understanding the impact reaction but are highly difficult to predict. This complexity makes terminal ballistics a highly challenging topic for modeling and analytical efforts. A detailed

description of all of the mechanisms of such an impact is beyond the scope of this thesis, but an abbreviated overview will be presented.

When a projectile strikes an armor plate, there are a number of possible results. The projectile may shatter or break upon impact, be deflected in a new direction, penetrate or perforate the plate, or any combination of these. Many factors control the outcome of such an impact, the most important of which are the velocity of the projectile and the mechanical properties of both the projectile and the plate.

Two possible outcomes of this sort of impact are ricochet and penetration, and the following sections will provide a brief introduction into these reactions.

2.4.1 Ricochet

Projectile ricochet has been the subject of much research [6, 7, 8, 9], but it is apparent that no authoritative and final model capable of providing a comprehensive understanding of ricochet dynamics has yet been developed [10]. Though not a comprehensive model, Tate [11] proposes a model useful in providing a rough prediction of the critical angle of obliquity above which angle projectile ricochet or break up is very likely to occur. This model is shown in Equation 2.3.

$$\tan^3 \psi_c = \frac{2}{3} \frac{\rho_p v_p^2}{Y_p} \left(\frac{l^2 + d^2}{ld} \right) \left(1 + \sqrt{\frac{\rho_p}{\rho_t}} \right) \tag{2.3}$$

Here, ψ_c is the critical angle of obliquity for ricochet, as shown in Figure 2.5. Additionally, ρ_p is the projectile density, v_p is the projectile's impact velocity, Y_p is the characteristic projectile strength (closely related to Hugoniot elastic limit of material), l and d are the projectile's length and diameter, respectively, and ρ_t is the target density.

This model was developed for long rods and makes several simplifying assumptions. Deceleration of the rod during impact is neglected, a square rod cross section is assumed, and Tate's modified hydrodynamic theory [12] is also assumed to be true. Based primarily upon a given set of values for projectile density, length-to-diameter (L/D) ratio, and strength, the critical ricochet angle can be calculated. Alteration of the parameters in

9
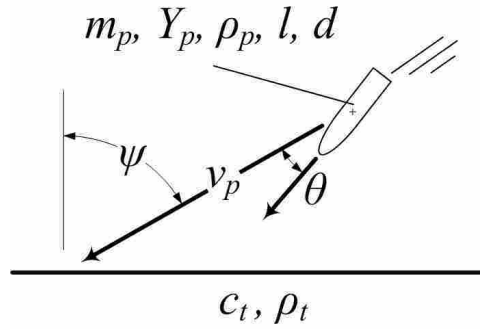
Figure 2.5: Projectile penetration parameters
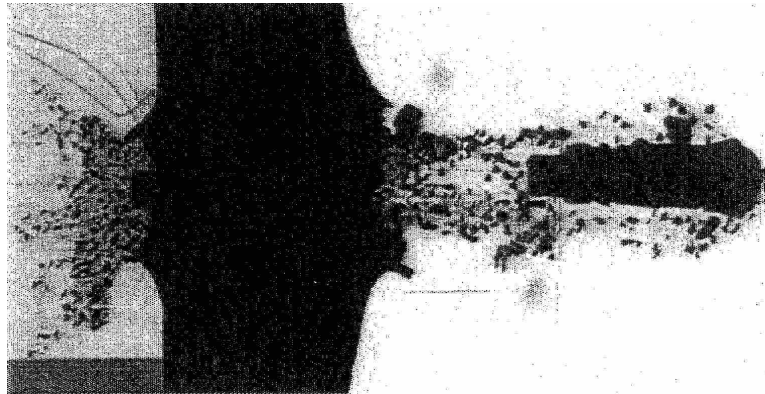
Figure 2.6: X-ray shadowgraph of impact of 25mm APDS projectile on alumina target [13]

this equation tend to have a small effect on the critical ricochet angle, ψ_c, because its tangent is a function of their cube root. In other words, for a given combination of projectile and armor plate, the critical angle of obliquity for ricochet is relatively insensitive to any change in these parameters [10].

2.4.2 Penetration

In the case of traditional armor systems consisting solely of solid plates, absorption of a projectile's kinetic energy by the system is primarily limited to that absorbed during penetration. When a ballistic projectile strikes and begins to penetrate an armor plate, energy concentrations in the plate are formed. These energy concentrations, in the form of strain energy, propagate through an impacted target as stress waves. Figure 2.6 shows an example of armor plate failure as a result of these stress waves.

10

Significant research efforts have been invested into developing a greater understanding of the processes and results of stress wave propagation during ballistic penetration into armor systems. The physics involved in these impact reactions are highly complex and not fully understood, but several empirically-based models have been proposed for predicting penetration behavior during impact.

For typical projectile and armor parameters, an illustrative model for penetration is offered by Stone [14]. He presents a simplified model for predicting a blunt-nosed projectile's depth of penetration during a normal impact into a semi-infinite slab of stable, structurally hard material. The model applies to the case without significant projectile deformation, yaw, or tumble, which equates to $\psi = 0$ and $\theta = 0$. The model is of the following form:

$$P = \frac{m_p v_p^2}{2\pi r_p^2} \frac{2}{\rho_t c_t} \tag{2.4}$$

where P is penetration depth, m_p is mass of the projectile, r_p is the projectile radius, and c_t is a parameter representing the target's mechanical properties. A KE weapon's penetration power is thus a function of its initial kinetic energy per unit of impacting surface area, and the target's mechanical properties. Other models for penetration will also be presented later in Chapter 8.

2.5 Ballistic Armor

As far back as the middle ages, armor designers have struggled to develop systems capable of defending against deadly ballistics. Figure 2.7 shows a suit of armor which originally rendered its wearer virtually invincible. Eventually, improved weapons like the crossbow made such armor obsolete. Similar advances in weapon technology have provided consistent pressure on armor designers to understand and defeat a wide range of weapons.

This section will introduce the primary threats to be addressed by CMRA systems, and the current trends in armor design.

Figure 2.7: Medieval plate armor

2.5.1 Threats

Modern armor for military vehicles must be able to withstand attacks from a variety of types of weapons. Most such attacks can be categorized as either kinetic energy weapons or explosive weapons.

Kinetic Energy Weapons

Kinetic energy (KE) weapons, also known as KE penetrators, are generally designed to concentrate a maximal level of kinetic energy into a minimal projectile cross section in order to result in the maximum penetration depth. Because the kinetic energy of a projectile is directly related to the mass of the projectile, weapon designers strive to increase the sectional density of the projectile, which is defined to be the mass per unit of cross sectional area. KE weapons with large velocities and sectional densities thus tend to be more successful. In the world of medieval plate armor, the success of the archer's arrow in penetrating armor came from the arrow's high velocity and narrow tip. Sharpened arrowheads such as that shown in Figure 2.8 provided an even greater sectional density for the arrow.

Armor-piercing fin-stabilized discarding sabot (APFSDS) rounds are a modern example of these same principles. Like other armor-piercing rounds such as that seen in

Figure 2.8: Sharpened medieval arrowhead

(a) Disassembled M993 7.62mm NATO standard armor-piercing round [15]
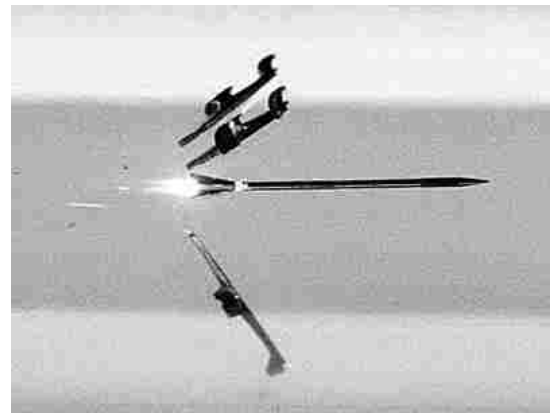
(b) APFSDS showing discard of sabot immediately after exiting the muzzle

Figure 2.9: Armor piercing kinetic energy-based weapons

Figure 2.9(a), the APFSDS is designed to be narrow and fast. In addition, the APFSDS manages to achieve much higher velocities and sectional densities through the use of a sabot. The sabot is a temporary housing for the projectile designed to increase the projectile's rear cross-sectional area during firing and then to be discarded after muzzle exit, as seen in Figure 2.9(b). In this way, firing pressures cause the greatest muzzle velocity and the least drag on the residual penetrator before final impact.

Explosive Weapons

Small-scale explosive weapons are increasingly common in modern warfare because of increased availability and decreased cost. These weapons rely on the timed release of ex-

plosive chemical energy to destroy a target. Rocket-propelled grenades and high-explosive anti-tank (HEAT) rounds are two common forms of explosive weapons.

Figure 2.10: High-explosive anti-tank (HEAT) round

There are similarities between armor systems designed to defeat both types of threats, but the CMRA systems discussed in this thesis center on defeating threats that are kinetic energy based as opposed to explosive in nature.

2.5.2 Armor Categorization

To succeed in defeating kinetic energy weapons, an effective ballistic armor system must be capable of preventing projectile penetration. This is generally accomplished by preventing any catastrophic energy concentration in the deceleration or deflection reaction. The wide variety of strategies for preventing this energy concentration can be categorized as shown in Figure 2.11.

As shown in the figure, vehicular armor technology can be divided between passive and reactive armor systems even though specific implementations of armor systems may overlap both categories simultaneously. These two categories of armor will be briefly introduced in the following sections.
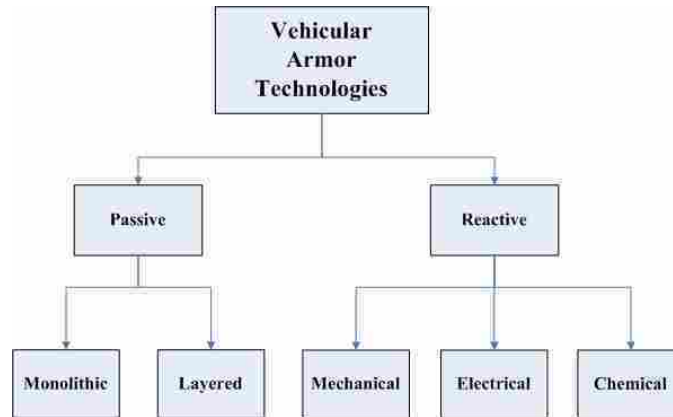
Figure 2.11: Ballistic armor categorization

2.5.3 Passive Armor

Passive armor is the most common and most traditional form of armor, and involves components that receive projectile kinetic energy without any form of active response. This type of system can be further categorized as either monolithic or layered armor.

Monolithic Armor

Monolithic armor is the most simple form of armor, in which a solid, homogeneous member is used as a buffer between a projectile threat and the item or person to be protected. This type of armor system is intended to reject a projectile's energy or absorb it through plastic flow, brittle fracture and/or heat generation [16]. Monolithic armor systems are advantageous for their simplicity, but are often inefficient in the face of modern KE weapons.

Layered Armor

Layered armor is a form of passive armor in which layers of monolithic plates are used in a single armor system. These layers tend to have different mechanical properties and desired functions in the impact reaction. It is common practice, for example, to employ thin, hard layers on the surface of armor systems to break up or shatter an incoming threat, and thicker softer layers behind the hard layer to absorb the fractured projectile's energy.

15

Layered armor systems are also used commonly in spacecraft shielding. The Whipple shield, as shown in Figure 2.12, employs a thin layer of aluminum located several inches away from the spacecraft hull as a disruption layer for hypervelocity projectiles such as micrometeorites. Rather than stopping a threatening micrometeorite, the aluminum layer vaporizes and disperses the mass of the micrometeorite. Even though the aluminum layer in a Whipple armor system tends to be perforated hundreds of times during its lifespan, the vaporized and dispersed projectiles have such diminished kinetic energy and sectional density that they rarely do any damage to the underlying spacecraft.

Figure 2.12: Whipple Shield (Courtesy NASA/JPL-Caltech)

Another form of successful layered armor is ballistic fabrics, such as the Kevlar® armor shown in Figure 2.13. Ballistic fabrics use woven layers of aramid fibers to spread the kinetic energy of the projectile as strain energy in as much of the mass of the armor as possible, avoiding the energy concentrations that lead to failure. Multiple layers of these fabrics are used to increased their efficiency.

2.5.4 Reactive Armor

Reactive armor differs dramatically from passive armor because it is capable of either releasing energy or transforming energy in such a manner as to minimize a KE weapon's ability to penetrate the system. Reactive armor is a recent development, with

Figure 2.13: Kevlar ballistic fabric

the first forms becoming available for common use only in the past few years. This type of armor can currently be divided between chemically or explosively reactive armor, electrically reactive armor, and mechanically reactive armor, as shown in Figure 2.14.
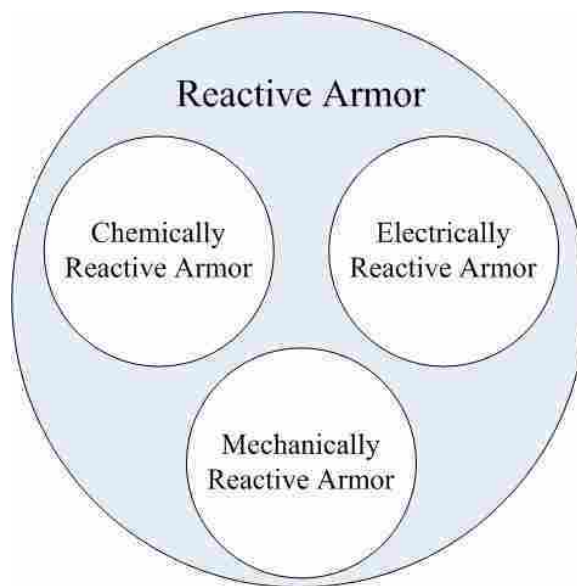
Figure 2.14: Reactive armor categorization

Chemically/Explosively Reactive Armor

The most common form of reactive armor is chemically or explosively reactive armor. In this type of armor system, small chemical-based explosives are mounted behind small armor plates covering the surface of the vehicle to be protected, as seen in Figure 2.15. When a weapon reaches the plates, the explosive is detonated and the plate accelerates into the threat, disturbing and often neutralizing it.

This strategy has turned out to be especially effective against HEAT weapons, as the plate and explosive tend to significantly disrupt the jet of high-pressure molten metal that would otherwise penetrate and destroy the vehicle.

Figure 2.15: Russian T-72 tank equipped with explosively reactive armor plates

Electrically Reactive Armor

Electrically reactive armor is similar to explosively reactive armor in that a large amount of energy is released into the threat in order to disrupt and defeat it. In electrically reactive armor, however, a series of charged, electrically conductive plates are utilized to release

18

tremendous levels of energy into penetrating weapons [17, 18]. Tens of thousands of amps of electrical current can reduce the threats from deadly to harmless before significant damage is done to the vehicle.

Mechanically Reactive Armor

As explained in the introduction, Mechanically Reactive Armor (MRA) is here defined to be a specialized subset of reactive armor systems. This subset is designed to minimize a kinetic energy projectile's penetration power by using a kinematic mechanism or linkage to effectively deflect or absorb its kinetic energy. In many cases, this is accomplished by harnessing the projectile's momentum and kinetic energy and submitting it to the motion of the primary armor mechanism.

Though it falls into a previously undefined category of armor, an example of MRA was patented by William F. Donovan in US Patent 5402704 [19] in 1995. As shown in Figure 2.16, a sacrificial armor plate is mounted with a hinge such that a penetrating projectile is released in a different direction than the original direction (γ being the change in trajectory). By "catching" the projectile and submitting it to the motion of the mechanism, this patent provides a greater angle of obliquity for some final armor impact.

Another example of armor that follows these same principles but is not precisely MRA is shown in Figure 2.17. Patented by Charles E. Anderson, Jr., Dennis L. Orphal, and Gordon R. Johnson [20], this concept places a small armor plate in the path of the projectile and allows the plate to "catch" the projectile, to detach from the supporting substrate and then to ultimately decelerate at some back surface.

It is also important to note that MRA presents great advantages when compared with other reactive armor in terms of safety. Both chemically and electrically reactive armor, as currently implemented, tend to be highly dangerous for friendly troops. Alternately, because it is constrained by the motion of its links, MRA is likely to be much more easily contained, even when containing significant levels of potential energy.
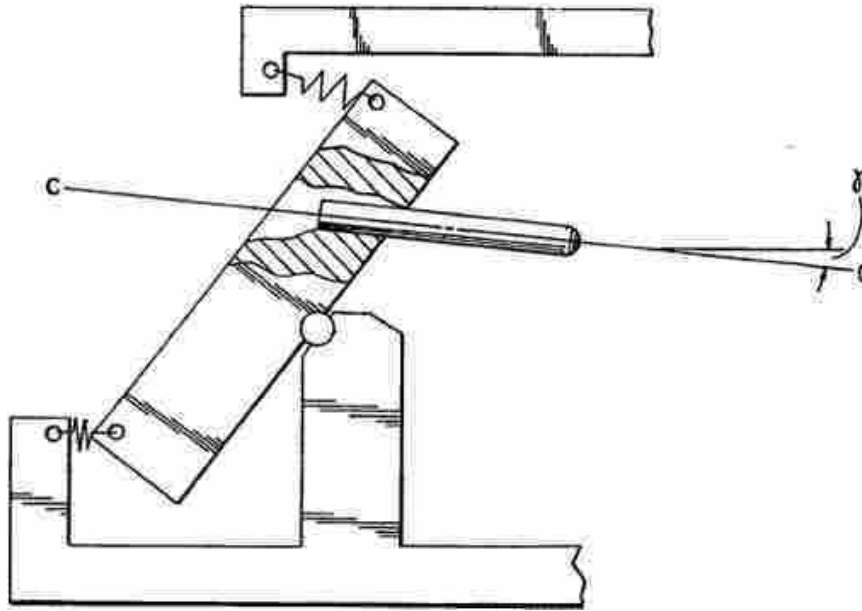
Figure 2.16: Image from US Patent 5402704 [19]

Compliant Mechanically Reactive Armor

As described in Chapter 1, Compliant Mechanically Reactive Armor, of CMRA, is a subset of MRA where the primary armor mechanism is compliant as opposed to rigid. In this way, the advantages of compliant mechanisms discussed previously are brought to bear in the design of demanding mechanical armor systems.

It is important to note that the mechanisms included in CMRA systems need not compose the entire armor system. The motion and behavior of the mechanism is likely to require small armor plates functioning in tandem with the mechanism. For this reason, CMRA *elements* are defined as the primary mechanisms of CMRA systems, which systems generally include traditional solid armor plates as well as the elements. This is demonstrated in Figure 2.18.

2.6   Summary

This chapter has provided a brief review of a portion of the literature relevant to this thesis. Later sections contain reviews of literature specific to the modeling performed. The discussion of rigid-body and compliant mechanism theory provides an important backdrop
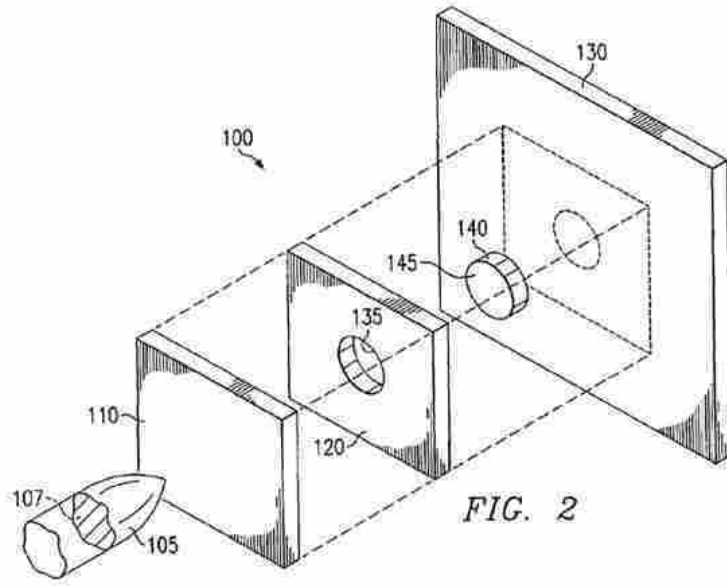
Figure 2.17: Image from US Patent 7077048 [20]
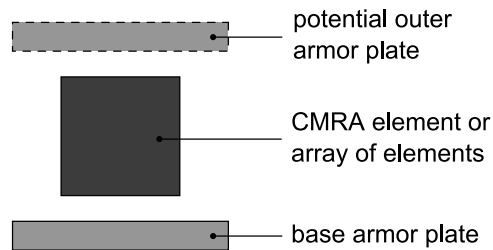
Figure 2.18: Potential CMRA system schematic demonstrating the inclusion of small armor plates in cooperation with the CMRA element, or primary mechanism

for the discussion of the design of CMRA systems. Because the elements of CMRA systems may be composed of rigid-body or compliant mechanisms, an understanding of the basic behavior of these mechanisms is critical to understanding the function of CMRA systems. The brief consideration of impact mechanics serves to identify the basic relationships at play in the operation of CMRA systems. Finally, the current state of ballistic armor technology is discussed and presented in order to map the location and relationships of MRA to other armor forms.

Chapter 3

Research Approach

3.1 Introduction

This chapter outlines the methodology used to accomplish the objectives of this thesis. Each of the steps of this methodology will be introduced in the following sections, and then detailed in the successive chapters. The steps are also shown in Figure 3.1. This methodology represents a modified version of several different design methodologies, including that presented by Ulrich and Eppinger [21].

3.2 Identification of Design Principles

To facilitate the creation of new ideas and to assimilate and synthesize existing ideas, a framework for thinking about and discussing the relevant topic must be developed. The first step in the design of CMRA elements involves the development of such a framework. In this case, the framework consists of a categorization of governing principles into which potential ideas must fall. These categories can then eventually be populated with concepts worthy of close investigation. This framework is crucial in that it allows comparison and contrast of different ideas, and directs thoughts in new directions.

The first step in the development of this framework involves drawing physical relations and equations from the relevant literature. Various texts dealing with the physics of collisions and impacts were consulted to provide a sound foundation for the research. Additional literature dealing specifically with the design of armor systems was also consulted, but unfortunately much of current armor technology and research is classified and unavailable. The majority of such literature focuses on providing advances in material science capable of improving the performance of passive armor systems, and is thus only of limited usefulness in identifying principles for mechanically reactive armor.
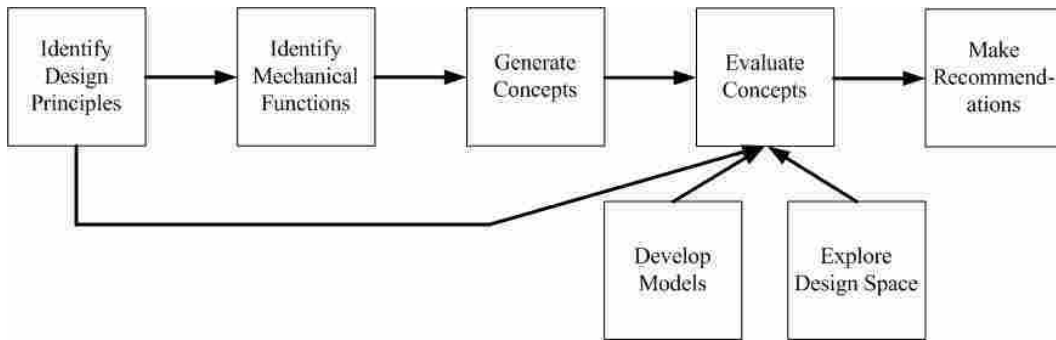
Figure 3.1: Research approach outline

Even so, there are several published sources that offer principles relevant to the design of armor. From these sources, which are detailed later, equations and relationships can be found which offer a valuable starting point for the design of mechanically reactive armor. The framework is then conveniently divided between ideas that modify different parameters in the terminal ballistic relationships in order to improve armor performance.

Even though this stage is quite likely the most challenging and broad of the entire design process, it is also the most important. All successful ideas are seeded in this early development. Chapter 4 will detail this stage of the research.

3.3 Identification of Mechanical Functions

After identifying these design principles and using them as categorizations in the research framework, a link is needed to tie the principles to specific concepts and ideas.

Drawing from mechanism theory, specific mechanical functions capable of providing the necessary change dictated by a design principle can be identified. These mechanical functions represent the actual physical means for providing the variation in the impact reaction required by the principles. In this sense, one mechanical function may easily satisfy more than one design principle as long as the behavior alters the corresponding input to the impact penetration reaction. This will be demonstrated in Chapter 5.

3.4 Concept Generation

After the mechanical functions have been identified, they can be used to map the design principles directly into specific theoretical and conceptual embodiments of CMRA elements. This stage consists simply of creating or synthesizing mechanisms capable of performing the mechanical functions identified earlier. Chapter 6 documents the CMRA concept generation.

In order to find mechanisms that would offer the required functions, both external and internal searches were performed.

3.4.1 External Search

Literature and Patent Search

Beyond the identification of the design principles mentioned above, peer-reviewed literature can also be an excellent source of ideas for concept generation. Even though much literature detailing the design of armor systems is proprietary or classified, some ideas can be found in the available literature. Because literature dealing with armor systems often tends to focus on analysis techniques, trends and patterns can be identified from the armor systems being analyzed.

In addition to a search of peer-reviewed literature, a search of patents can offer a great profusion of ideas. These ideas must often be carefully examined since patents are not peer-reviewed and may not actually function as purported.

Benchmarking

Similar to the search of patents, benchmarking is the "study of existing products with functionality similar to that of the product under development"[21]. This study can reveal ideas and solutions that have been used in similar and related fields. Even though other fields of technology may appear totally unrelated to the field of the product under development, they may still house insightful solutions that can be applicable. In the case of armor systems, related fields of technology involve any products and concepts that absorb energy, dissipate energy, spread energy, or resist damage during impact.

3.4.2 Internal Search

Building on the ideas found during the external search, an internal search is used to identify new and original concepts. Closely related to brainstorming, the internal search seeks to create and synthesize ideas by concentrated generative effort.

3.5 Concept Evaluation

The goal of the evaluation stage consists of two main efforts. The first effort is to judge the relative probability of success of the different concepts using concept screening. Concept screening focuses on the narrowing of the broad group of original ideas into a select and tractable group for closer evaluation. Screening utilizes qualitative comparison and ranking procedures to identify the subset of concepts most likely to succeed and most worthy of further evaluation. The qualitative comparison focuses on using the design principles developed earlier as screening criteria.

The second effort is determine preliminary quantitative measures of the success of the narrowed concepts and to identify trends within the design space of these concepts. These quantitative measures rely on the development of models capable of shedding insight into the complex behavior of CMRA elements during ballistic impact. The development and validation of the full simulation model used in this thesis is detailed in Chapter 8.

The second effort also entails a rough analysis of whether or not the concepts are actually feasible and practical in terms of actual physical materials and dimensions.

3.6 Summary

The research methodology and approach used in this thesis to accomplish the thesis objectives has been presented and detailed. The essential steps in this methodology involve identification of CMRA design principles and mechanical functions, as well as the generation and evaluation of CMRA concepts.

Chapter 4

Design Principles for Mechanically Reactive Armor

4.1 Introduction

The observations and models introduced previously give rise to a number of design principles of use to armor designers. These principles are focused upon using mechanical means to modify the parameters of interest in the physical impact phenomena discussed earlier. Each principle represents an approach to the successful performance of the MRA or CMRA system.

The performance of a MRA or CMRA system can be measured in terms of its ability to prevent damage. First and foremost must be the protection of the items or persons to be shielded by the armor and second is the minimization of damage to the armor system itself. Because of the added complexity of MRA and other reactive armor systems, the system's performance must justify the added costs by demonstrating increased mass efficiency. This performance and efficiency increase may consist of reduced weight requirements with equivalent armor performance and ballistic limits, or of equivalent weight requirements with improved armor performance and ballistic limits. For the case of an armor system like that shown in Figure 2.18, this equates to one of two requirements:

1. The outer armor plate must experience less projectile penetration than would a simple solid armor plate of equivalent mass, or

2. The outer armor plate must experience equivalent projectile penetration to a simple solid armor plate of greater mass.

In order to reduce projectile penetration, then, the variables in Equation 2.4 must be altered by the MRA or CMRA element. The principles and design approaches composing this section are drawn from the basic changes which make reduced penetration possible.

Table 4.1: Mechanically reactive armor design principle families

Family	Design Principle
Energy Rejection	Ricochet induction
Energy Minimization	Obliquity
	Relative velocity reduction
Energy Dissipation	Transfer rate minimization
	Strain energy distribution
	Sectional density reduction
	Rotational or lateral kinetic energy transfer

The principles or approaches are organized into newly defined families of similar methods. Each of the three families are introduced and populated in the following sections. Table 4.1 displays a summary of these families as well as the principles that make up each family.

4.2   Energy Rejection Family

The first family to be discussed is entitled Energy Rejection. In this family, some or all of the energy of the incoming projectile is rejected from the armor system without transfer into the system. By rejecting the energy in this manner, the armor system is spared the challenge of safely absorbing the concentrated burst of energy from the projectile. This results in the least residual damage to the armor system, as well as the greatest capacity for withstanding repeat hits.

4.2.1   Ricochet Induction

As explained before, rejection of the majority of a projectile's energy generally requires ricochet or break up. To mechanically enhance an armor system's ability to reject incoming kinetic energy by ricochet, the impacting surfaces must be obliquely oriented at or above the critical angle for ricochet. Critical ricochet angles tend to be rather large, and sufficient obliquity requires significant plate rotation.

One challenge with ricochet induction is that the projectile's path is generally not significantly affected and using ricochet to redirect a projectile away from a target to be protected may require multiple ricochets.

4.3 Energy Minimization Family

In the Energy Minimization Family, when a projectile's kinetic energy cannot be rejected, mechanical means can be used to minimize the effective magnitude of the incoming energy.

4.3.1 Obliquity

By increasing the angle of obliquity, even when ricochet or break up cannot be achieved, the component of the projectile's velocity normal to the impacted target or plate is reduced. Alternatively, the plate's effective thickness is increased because the projectile must penetrate the target at an angle, as shown in Figure 4.1.

Also known as "sloped armor", this is a generally accepted armor design, and has been employed in much of the armor used on heavy tanks (see Figure 4.2).
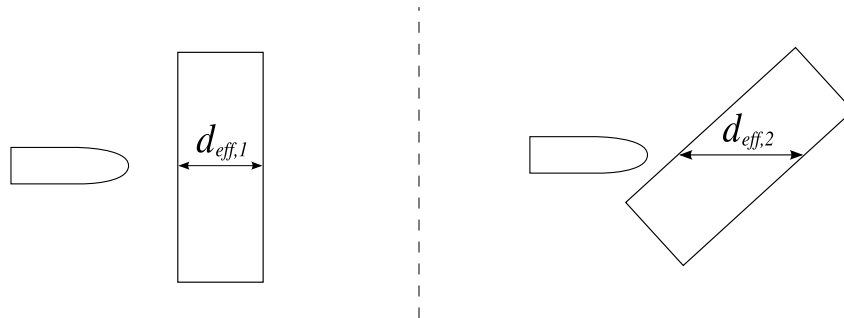
Figure 4.1: The effect of impact obliquity on effective plate thickness; note that $d_{eff,1}$ is less than $d_{eff,2}$

4.3.2 Relative Velocity Reduction

Because the most critical parameter in predicting penetration depth is the impact velocity of the projectile, any mechanical means of reducing the relative velocity between the projectile and the armor prior to impact would reduce penetration. Spaced armor, or armor which places sacrificial preliminary armor layers some distance from a base armor plate, is intended to decelerate, disturb, and possibly even disintegrate the projectile prior

Figure 4.2: 1941 Soviet T-34 tank with sloped armor

to impact with the base armor. This is the principle motivating the design of the Whipple shield and its variations in spacecraft shielding, as mentioned previously.

Another method of minimizing the relative velocity between projectile and armor would be to initiate velocity in the impacted component of the armor prior to or during impact. If the armor plate could reach a velocity composing at least a significant fraction of the impacting projectile's velocity, total impact penetration could be reduced prior to or during the final deceleration of the projectile. To be effective, this would likely require the release of significant amounts of energy stored within the armor system as well as a very light armor plate.

4.4 Energy Dissipation Family

When the incoming kinetic energy cannot be rejected and its effective magnitude has been minimized, the remaining energy must be absorbed by the armor system. As mentioned earlier, this has traditionally been accomplished by the mechanical deformation of some plate. Any amount of energy absorbed by other mechanical means or components will reduce the energy absorption requirement imposed on the armor plate, and may therefore reduce the projectile's penetration into the base plate.

4.4.1 Transfer Rate Minimization

The impulse-momentum change relationship (Equation 4.1) applied to a ballistic impact states that in transferring a projectile's momentum to the target in a perfectly inelastic collision, the impacted mass or "target" must supply an impulse to the projectile sufficient to decelerate the projectile and accelerate itself to a common velocity.

$$m\Delta v = F\Delta t \qquad (4.1)$$

Here, m is the mass of the projectile, Δv is the change in the velocity of the projectile during the impact, F is the impact force, and Δt is the impact duration.

From this equation, it can be seen that impact forces in the target, and their accompanying stress waves, are a function of the total time required to decelerate the projectile completely. Maximizing this time duration, or minimizing the energy transfer rate, will reduce penetration distance and can be accomplished mechanically by decreasing the effective stiffness of the impacted plate. This effective stiffness is a function of the material properties, geometry and boundary conditions of the target.

4.4.2 Strain Energy Distribution

Because mechanical deformation results when the magnitude of induced stress waves in the target meet or exceed the material strength, reduction of the magnitude of these stress waves will result in less deformation and penetration. Stress wave magnitude in an isolated mechanical system is inversely related to the amount of mass involved in the reaction. The success of ballistic fabric armor systems, often composed of layers of woven aramid fibers such as Kevlar®, is due in part to the spreading of impact loads over significant portions of the mass of the fabric. This same principle applies to other armor systems. An increase in the total quantity of mass involved in bearing the stresses induced during impact results in a lower maximum magnitude of stress, and less projectile penetration.

In normal operating conditions, only a very small fraction of a total armor system is likely to be impacted, and the vast majority of the mass of any traditional plate armor

31

system will be unused. In this case, large measures of strain energy storage capacity are wasted, and therefore any method for utilizing a greater proportion of this capacity will result in greater armor efficiency. Spreading this strain energy may occur if energy is distributed laterally upon impact or if the projectile's effective contact area is increased through deformation, augmentation, yaw, or tumble.

4.4.3   Sectional Density Reduction

Closely related to the principle of efficient distribution of strain energy during impact is the principle of decreasing the projectile's sectional density. As clarified above, the penetration power of a projectile is related to its kinetic energy per unit of impacting surface area. Penetration, therefore, can be reduced by minimizing the ratio of projectile mass per unit of impacting surface area, or projectile sectional density. As before, this can be accomplished by inducing projectile instability or yaw, or by reducing the L/D ratio of the projectile.

4.4.4   Rotational and Lateral Kinetic Energy Transfer

Dissipation of a projectile's kinetic energy may also take place in a transformation to rotational or lateral kinetic energy. Because energy is conserved, any energy spent causing rotation during impact cannot be used in deforming and penetrating a target. Additionally, any armor element that undergoes lateral motion (that is, motion which is parallel to the plane of the armor) during impact likewise removes penetration power from a projectile. The incorporation of an armor element capable of absorbing a projectile's kinetic energy as rotational or lateral kinetic energy provides a harmless reduction in penetration. It should be noted that this principle differs from the distribution of strain energy in that it focuses on inducing *motion* in a secondary direction (lateral or rotational) rather than simply in spreading the stress in a secondary direction.

4.5   Summary

This section has provided a foundation for exploring the design of CMRA systems. Drawing from the ballistic impact relationships identified in Chapter 2, a number of design

32

principles and approaches of use to armor designers have been identified. The principles are categorized into the Energy Rejection family, Energy Minimization family, and the Energy Dissipation family. Each design principle is directly tied to the alteration of parameters upon which the predictive impact relationships depend.

Chapter 5

Mechanical Functions

5.1 Introduction

The principles outlined in Chapter 4 serve as an important foundation for the remainder of this research. MRA or CMRA systems that will be successful in improving armor efficiency inasmuch as they manage to follow the approaches outlined previously.

In order for a certain MRA or CMRA concept to follow the specific approaches from Chapter 4, it must supply certain functions. These functions are the actual mechanical behaviors of an element which incites projectile ricochet, strain energy distribution, etc.

This section will outline the specific mechanical functions that directly satisfy each of the aforementioned design principles. The families, principles and the related mechanical functions are summarized in Table 5.1. These functions will be discussed in the following sections.

Again, it should be noted that the functions discussed here are applicable to both rigid-body and compliant MRA systems because both are capable of providing these functions.

5.1.1 Armor Plate Orientation

The most simple of the functions to be discussed is that of armor plate orientation. In order to provide greater opportunity for ricochet induction (Section 4.2.1) and impact obliquity (Section 4.3.1), the CMRA element must be capable of positioning the impacted armor plate at a desirable angle. This could be performed before and/or even dynamically during the impact as long as the effective angle of obliquity is increased.

Table 5.1: Mechanically reactive armor design principles and required functions

Family	Design Principle	Related CMRA Function
Energy Rejection	Ricochet induction	Armor plate orientation
Energy Minimization	Obliquity	Armor plate orientation
	Relative velocity reduction	Accelerated elements
Energy Dissipation	Transfer rate minimization	Controlled stiffness
	Strain energy distribution	Lateral array, controlled stiffness
	Sectional density reduction	Accelerated elements
	Rotational or lateral KE transfer	Armor plate orientation, lateral array

There are a great many mechanisms which are capable of specific motion and positioning functions. One example is the common four-bar hinge mechanism, shown in Figure 5.1, which is often used for doors or other rotating members.
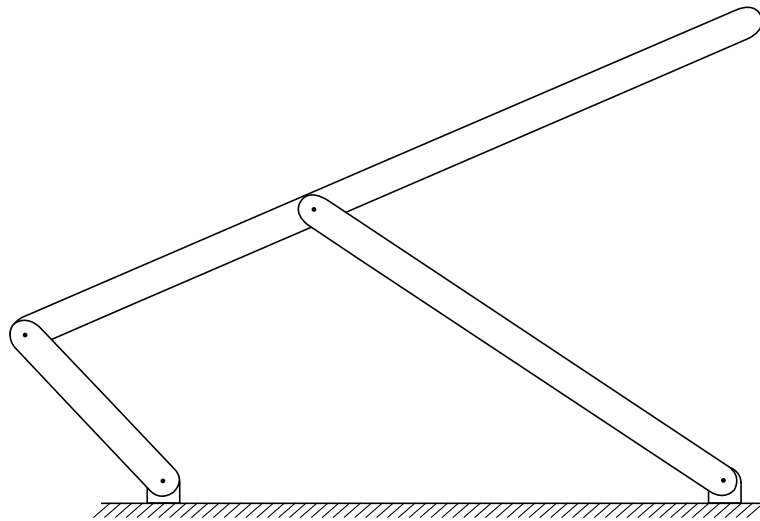
Figure 5.1: Four-bar hinge mechanism

5.1.2 Controlled Stiffness

Controlling the stiffness of the impacted plate directly satisfies the principle of transfer rate minimization (Section 4.4.1). Different configurations of compliant mech-

anisms provide a wide variety of stiffnesses. Compliant mechanism synthesis allows a designer to specify a desired force-deflection relationship and create a mechanism to provide the desired relationship. A designer can also influence the inertial characteristics of the mechanism, which play a significant role in stiffness during impact. This freedom allows a designer to optimize the dynamic stiffness of a CMRA element to deliver optimal penetration resistance.

Controlled-stiffness mechanisms are common in many different applications. One example is the constant force mechanism shown in Figure 5.1.2. This mechanism, when designed properly, resists motion with a constant force throughout its displacement.
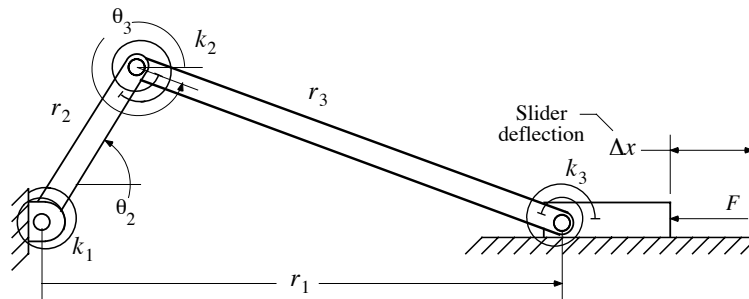
Figure 5.2: Constant force mechanism [5]

5.1.3 Accelerated Elements

Unlike rigid-link mechanisms, compliant mechanisms store and release potential energy in their beams during deflection. Thus, in a deflected state, such a mechanism is capable of releasing stored energy and causing accelerated motion. Such a mechanism is commonly called a cocked mechanism. Cocked mechanisms are not a recent invention and can be found among the sketches of Leonardo Da Vinci. The crossbow ballista shown in Figure 5.1.3 is one example.

The "spring-loaded" property of cocked mechanisms can be used to the advantage of an CMRA system if the stored energy can be released in such a manner as to reduce the relative velocity of a projectile prior to impact or to assist in providing a controlled stiffness
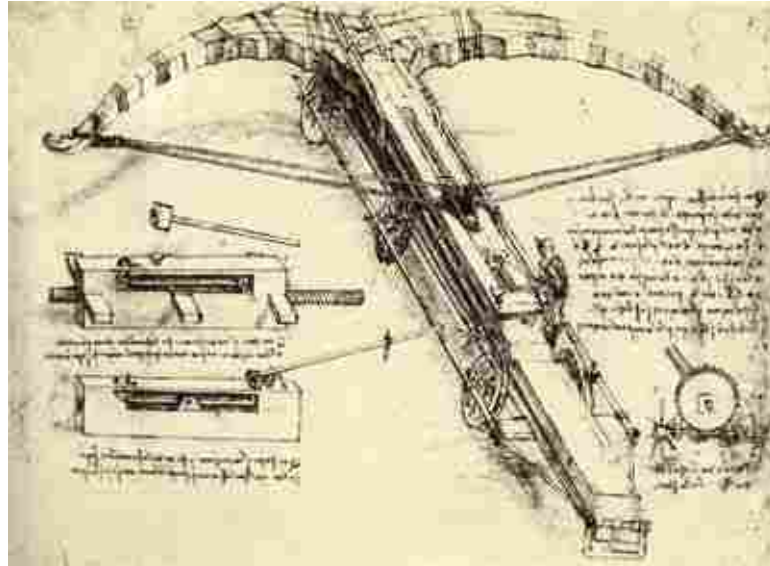
Figure 5.3: Crossbow ballista from the sketches of Leonardo Da Vinci (Courtesy Sandia National Laboratories)

as mentioned above. Additionally, when combined with the armor plate rotation mentioned previously, cocked CMRA elements could potentially be used to induce projectile yaw, and thereby diminish penetration. In this way, a cocked mechanism could satisfy the principles of relative velocity, transfer rate minimization, and sectional density reduction.

5.1.4 Arrays of Elements

Compliant mechanisms lend themselves well to the design of armor systems composed of interconnected arrays of independent elements. Because of their inherent flexibility, an array of interconnected compliant mechanisms could form a mechanical system much like the ballistic fabrics discussed earlier (see Figure 5.4). Not only could such an array of elements distribute impact strain energy among the masses of the individual elements and disperse energy rotationally or laterally, but the advantages offered by the other MRA principles could also be applied separately by each element. In this way, arrays of these CMRA elements could satisfy all of the principles listed in Table 4.1.

Figure 5.4: Kevlar ballistic fabric

5.2 Summary

This section presented the mechanical functions capable of satisfying the design principles outlined in the previous chapter. These functions are armor plate orientation, controlled stiffness, element acceleration, and array combinations.

Chapter 6

Concept Generation

6.1 Introduction

The principles and functions previously outlined give rise to specific concepts which will be outlined in this section. This section describes the concepts resulting from the concept generation process.

6.2 Concepts

The following concepts are the specific embodiments of CMRA elements resulting from the forgoing research methodology. These concepts are offered as illustrations of mechanisms capable of providing one or more of the functions required by the principles described earlier and shown in Table 5.1.

6.2.1 Emergent Four-Bar

The mechanism shown in Figure 6.1 consists of a partially compliant four-bar mechanism with an armor plate serving as the coupler. The mechanism transforms so that the coupler may lie in the same plane as ground or a base armor plate. During transportation or storage, the mechanism could be positioned in this transformed, retracted state, and then deployed in the extended state during operation. A similar mechanism is displayed in Figure 6.2. Here, the compliant segments buckle during transformation and deflection. Either of these two concepts could be designed with armor plate geometry capable of providing increased impact obliquity (i.e. pointed plates).

These concept could be designed to provide the following mechanical functions:

- Armor plate orientation

- Controlled stiffness

- Lateral array
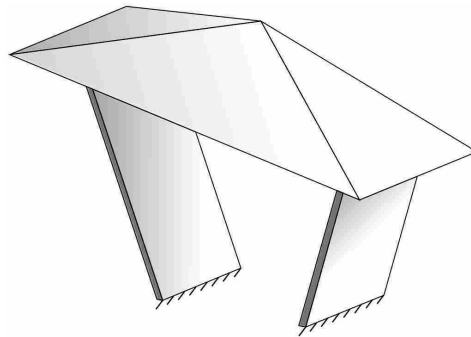
Figure 6.1: Emergent four-bar mechanism with armor plate coupler
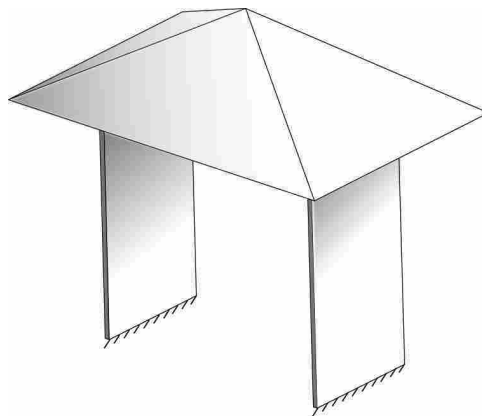
Figure 6.2: Buckling four-bar mechanism with armor plate coupler

6.2.2 Buckling Cantilever

A variation of the emergent four-bar mechanism is the cantilevered beam shown in Figure 6.3. This mechanism would behave in a similar manner to the buckling four-bar, except the armor plate would experience less resistance to rotation.

The buckling cantilever could be designed to provide the following mechanical functions:

- Armor plate orientation

- Controlled stiffness

- Lateral array
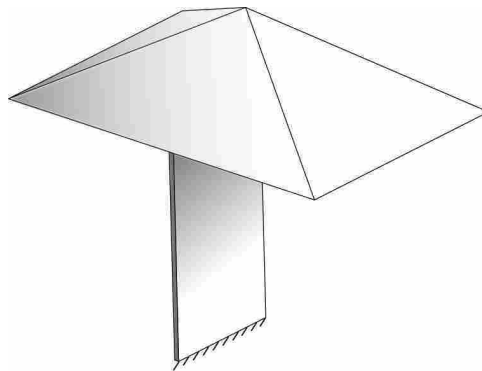
Figure 6.3: Buckling cantilever mechanism with armor plate attached

6.2.3 Cocked Four-Bar

The mechanisms displayed in Figures 6.1 and 6.2 could also be designed with different parameters to provide the "spring-loaded" effect which is characteristic of cocked mechanisms. Such a mechanism could be located beneath some outer armor plate, and then cocked such that the mechanism is extended vertically away from ground. Then, upon impact, internal energy in the compliant beams is released by accelerating the armor plate in line with and in the same direction as the impacting projectile, resulting in a lower relative velocity and a decreased effective initial resistance to the projectile.

This concept can thus provide:

- Accelerated elements

- Controlled stiffness

- Lateral array
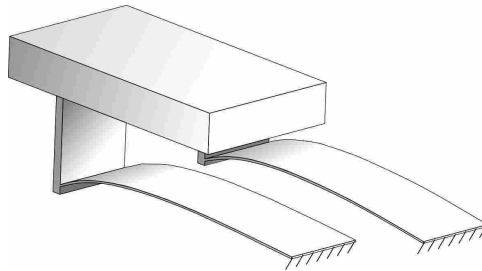
Figure 6.4: Cocked four-bar mechanism with armor plate coupler (shown in cocked position)

6.2.4 Cocked Cantilever

Similar to the cocked four-bar is the cocked cantilever shown in Figure 6.5. Here, the cantilever beam is fitted with a light armor plate at the free end to allow the plate to deflect with the beam.
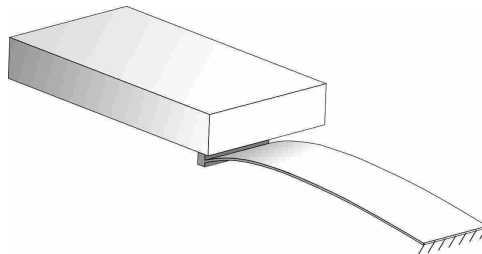
Figure 6.5: Cocked cantilever mechanism with armor plate attached to free end (shown in cocked position)

Like the Cocked Four-Bar, the Cocked Cantilever can provide:

- Armor plate orientation

- Accelerated elements

- Controlled stiffness

- Lateral array

6.2.5 Bistable Shuttle

The mechanism shown in Figure 6.6 consists of a bistable, partially compliant sliding mechanism with an armor plate slider. For bistability, the mechanism would be rigidly fixed at both ends of the thin compliant segments. This mechanism could be designed so that when it is positioned in one of the two stable slider positions, significant potential energy is stored in the compliant segments and only minimal force is required to switch the mechanism to the other stable state.

By positioning the stable position with the greater potential energy facing toward an incoming projectile, as shown in the figure, a nonlinear and initially low effective stiffness would be provided during impact.

If designed properly, this mechanism could provide:

- Armor plate orientation

- Accelerated elements

- Controlled stiffness

- Lateral array
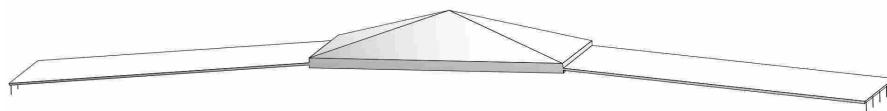
Figure 6.6: Bistable mechanism with armor plate shuttle

6.2.6 Buckling Tube

The mechanism displayed in Figure 6.7 consists of a linear spring, cylinder, or tube with a notch in one side. When mounted with an armor plate on the top surface and impacted, this tube could undergo a controlled buckling reaction which would provide:

- Controlled stiffness

- Lateral array
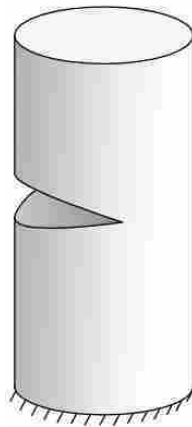
Figure 6.7: Notched tube for controlled buckling

6.2.7 Helical Rotating Spring

The mechanism displayed in Figure 6.8 consists of an armor plate mounted to several initially-curved compliant beams which are mounted to a base armor plate. Such a mechanism could be designed so that the armor plate would rotate during deflection, removing kinetic energy from the impacting projectile. In the case of perforation, where the projectile penetrates completely, this design also provides a spaced arrangement for projectile disturbance before final impact.
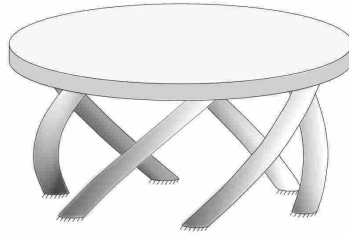
Figure 6.8: Helical rotating spring concept with armor plate above

This concept can provide:

- Accelerated elements

- Controlled stiffness

- Lateral array

6.2.8 Array Combinations

Any of the concepts discussed earlier could potentially be combined into arrays. As shown in Table 4.1, arrays of CMRA elements offer great advantages in the combination of several armor-enhancing functions. Two examples are shown here.

The systems displayed in Figure 6.9 consist of arrays of three different concepts. These mechanisms could be stacked laterally and/or upward out of the plane of a base armor plate. These arrangements of mechanisms could be used to mate the controlled stiffness, spacing, rotation, lateral motion, and projectile disturbance offered the individual concepts with the strain energy distribution of arrays of elements. These mechanisms can further be coupled with one another so that as one mechanism is actuated during impact, the others are actuated in turn.

6.3 Summary

Following established concept generation methodology, several concepts have been generated which directly satisfy the design principles and mechanical functions explained
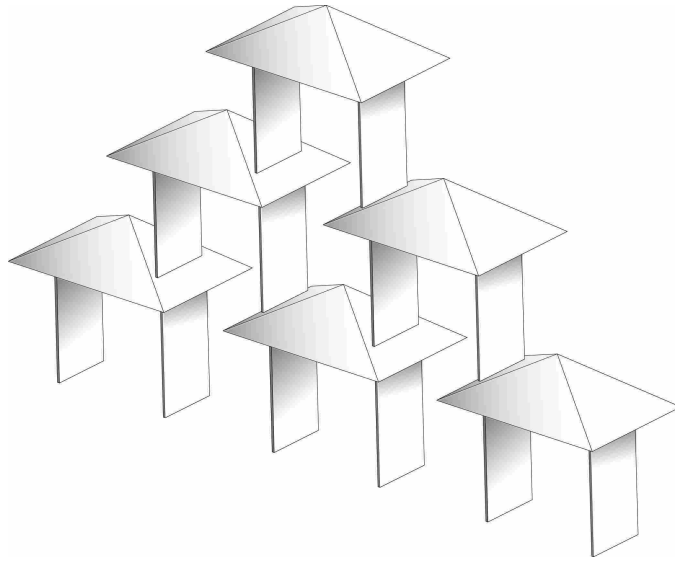
(a) Buckling four-bar mechanisms
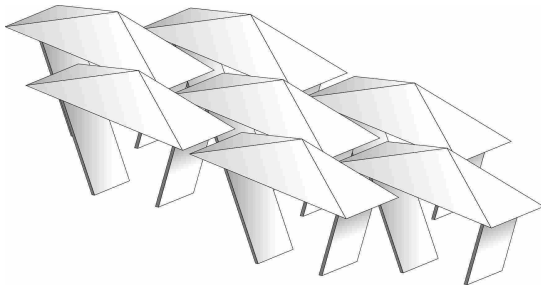
(b) Emergent four-bar mechanisms

(c) Helical rotating spring mechanisms

Figure 6.9: Array combinations

in Chapters 4 and 5. As explained, the concepts can be combined into arrays where their functions are coupled for improved performance.

Chapter 7

Concept Evaluation

7.1 Introduction

This section presents the first steps in the process of concept evaluation in order to determine which concept families are most likely to reduce the overall deformation of the plate during impact. First, concept screening is used to narrow the group of concepts by comparing them qualitatively to one another. In the succeeding sections, quantitative models are developed to provide more in depth simulations of concept performance and to identify trends within the design space of specific concepts.

7.2 Concept Screening

In order to narrow the group of candidate concepts generated in the previous chapter, established screening methodologies are used. Drawing from Ulrich and Eppinger [21], there are four steps to be performed in CMRA concept screening.

1. Prepare the selection matrix

2. Rate the concepts

3. Rank the concepts

4. Select one or more concepts

The following sections will outline these steps as explained by Ulrich and Eppinger.

7.2.1 Prepare the Selection Matrix

The first step of the screening process involves comparing the rough, initial concepts to a reference concept using a screening matrix. This provides a rough relative measure of the probable success of individual concepts. The criteria used to evaluate the concepts in this screening stage consist of the basic mechanical functions identified in Chapter 5, as well as other criteria based on future feasibility and analysis. After gathering the concepts and the selection criteria, they are used to populate the matrix, as shown in Table 7.1. The proposed concepts are arrayed along the upper row and the criteria down the left column.

7.2.2 Rate the Concepts

After setting up the screening matrix, the concepts are rated in comparison to a single reference concept. In this case, the angled four-bar serves as the reference and the other concepts are rated on a scale from one to five, as shown in Table 7.2. The specific ratings shown in Table 7.1 were selected as the result of consultation with the BYU Compliant Mechanisms Research Group and others.

Each selection criterion is given a respective weighting corresponding to its relative importance. These weightings are then multiplied by the ratings for each concept, resulting in a weighted rating. In this case, the weightings are appropriately focused to reflect the likely importance of the mechanical functions and the feasibility for evaluation purposes.
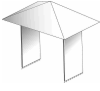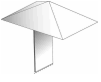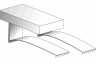
7.2.3 Rank the Concepts

After the weighted ratings are calculated, the concepts are ranked according to these ratings. In this case, the Cocked Cantilever and Helical Rotating Spring are the highest rated concepts.

7.2.4 Select One or More Concepts

Because the Cocked Cantilever and Helical Rotating Spring are the highest rated concepts, these are selected for further evaluation and simulation in the following chapters.

Table 7.1: Concept screening matrix; unweighted ratings range from 1 (low) to 5 (high)

		Concepts														
		Emerg. Four-Bar		**Buckl. Four-Bar**		**Buckl. Cantilever**		**Cocked Four-Bar**		**Cocked Cantilever**		**Bistab. Shuttle**		**Buckl. Tube**		**Helical Rot. Spring**	
Selection Criteria	**Weight**	Rating	Weighted	Rating	Weighted	Rating	Weighted	Rating	Weighted	Rating	Weighted	Rating	Weighted	Rating	Weighted	Rating	Weighted
Armor Plate Orient.	12%	3	0.36	2	0.24	2	0.24	3	0.36	3	0.36	1	0.12	2	0.24	2	0.24
Contr. Stiffness	20%	3	0.6	3	0.6	3	0.6	4	0.8	4	0.8	2	0.4	1	0.2	4	0.8
Armor Plate Accel.	3%	3	0.09	1	0.03	1	0.03	4	0.12	4	0.12	4	0.12	1	0.03	2	0.06
Array Compat.	10%	3	0.3	3	0.3	3	0.3	3	0.3	3	0.3	3	0.3	4	0.4	4	0.4
Mass Effic.	10%	3	0.3	2	0.2	3	0.3	3	0.3	4	0.4	3	0.3	3	0.3	2	0.2
Manuf / Assemb	10%	3	0.3	3	0.3	3	0.3	3	0.3	4	0.4	4	0.4	2	0.2	2	0.2
Ease of Analysis	35%	3	1.05	1	0.35	2	0.7	3	1.05	4	1.4	2	0.7	2	0.7	4	1.4
Total Score			3		2.02		2.47		3.23		3.78		2.34		2.07		3.3
Final Rank			4		8		5		3		1		6		7		2

Table 7.2: Concept screening rating scale

Relative Performance	Rating
Much worse than reference	1
Worse than reference	2
Same as reference	3
Better than reference	4
Much better than reference	5

7.3 Summary

This section has outlined the concept screening procedures recommended by Ulrich and Eppinger, and has established the necessity of developing quantitative models for further evaluation.

Chapter 8

Model Development

8.1   Introduction

After narrowing the concepts in the previous section, further evaluation and simulation are required to shed more insight into the behavior of the selected concepts. This next level of evaluation and simulation requires the development of a model that is capable of providing quantitative, independent behavioral simulations of CMRA systems during ballistic impact. Because the purpose of the evaluation is primarily to compare concepts and identify trends within the design space, parsimonious and tractable models are most desirable. Additionally, in order to illuminate the most general trends within the design space of the selected concepts, a generalized version of the concepts is used.

8.1.1   Generalized Concept: Spring and Damper
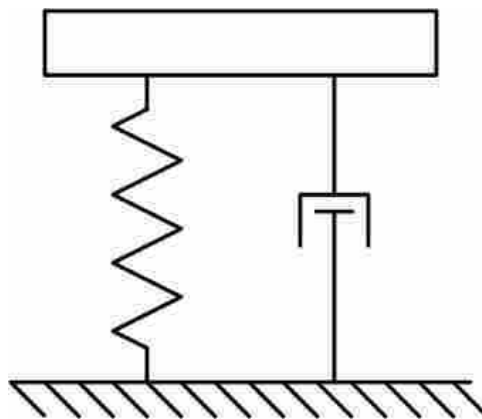
Figure 8.1: Spring and Damper concept with spring and damper mounted between armor plate and ground

The generalized concept, shown in Figure 8.1, consists of an armor plate mounted with a spring and damper on the backside. The damper, by definition, resists motion proportionate to the motion's velocity. The relation governing its force is shown in Equation 8.1, where b is the damper coefficient, $\dot{x}$ is the damper's velocity, and m is a constant exponent. The damper becomes nonlinear when $m \neq 1$.

$$F = b\dot{x}^m \tag{8.1}$$

Similarly, the spring resists deflection proportionate to its deflection from its resting state. One form for the equation governing the force produced by a spring is shown in Equation 8.2, where k is the spring coefficient, x is the spring's deflection, and n is a constant exponent. Again, the spring becomes nonlinear when $n \neq 1$.

$$F = kx^n \tag{8.2}$$

This concept, with its variable spring and damper, is capable of approximating the force-deflection curves of many of the other concepts, and thus is the most general concept.

This chapter will present several different evaluation methods before selecting one for use in simulating impact into this general concept.

8.2 Evaluation Model Comparison

The concepts generated and selected in previous chapters all incorporate some armor plate into a mechanical system. When the proposed CMRA element is successful in affecting the overall impact reaction, two separate behaviors are coupled together. A model capable of providing the necessary element evaluation can thus be decomposed into these two main components, as shown below.

- The **projectile-plate interaction** includes the elastic and plastic energy reactions, the momentum transfer, and the projectile penetration into the plate. This

| Finite Element Model | Lumped Parameter Model | Fluid Dynamics Force History Model | Linearized Force History Model | Initial Velocity Model |
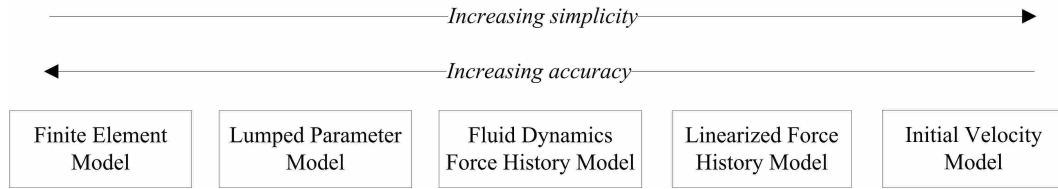
Figure 8.2: Several options available for modeling the projectile-plate interaction

interaction represents the highly complex impact phenomena that have been the primary subject of research of the field of terminal ballistics.

- The **plate-mechanism interaction** consists of the reaction between the stiffness-controlling element and the plate as it experiences the projectile's impact. The coupling between the two reactions occurs as the force and motion reaction of the plate from the projectile-plate interaction are imposed on the plate in this reaction.

Many different modeling approaches are available for shedding insight into both of the component reactions involved in decomposed overall system. Several of these options are displayed in Figure 8.2 and discussed in the following sections in order of increasing simplicity.

8.2.1 Finite Element Model

The most exact approach currently available for modeling a full CMRA system is the finite element (FE) method. In this method, the complexities of the shape, composition, thermal and mechanical properties, vibration, and energy response of both the projectile and CMRA elements can be accounted for. Such an approach could provide models for both the projectile-plate interaction and the plate-mechanism interaction.

Unfortunately, even though FE methods are extremely useful for gaining information about one specific design, the time investment required to develop and solve the model can be inhibitive. This is especially true in the early design phase, when general trends and behavior are much more valuable than one specific model's performance.

8.2.2 Lumped-Parameter Model

Another modeling approach that is much more useful in the early design phase is the use of lumped-parameter models. It is standard practice to employ lumped-parameter models to simplify complex phenomena into tractable predictive models for preliminary design and analysis purposes. In contrast to FE models, lumped-parameter models of mechanical systems such as the one displayed in Figure 8.3 consist of simplified elements such as massless springs and dampers, point masses, and idealized forces and impulses. The dynamic behavior of lumped-parameter models is governed by differential equations that can be solved analytically or numerically.
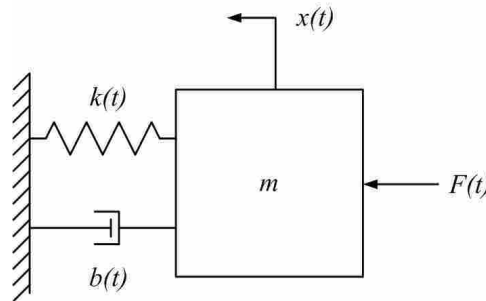
Figure 8.3: Simple lumped-parameter mass-spring-damper model

The governing equation for the model shown in Figure 8.3 is

$$m\ddot{x} + b\dot{x} + kx = F \tag{8.3}$$

where m is a point mass, b is a linear damping coefficient, k is a linear spring constant, and x, $\dot{x}$, and $\ddot{x}$ are the mass displacement and its first and second derivatives, respectively.

For CMRA analyses, lumped-parameter models could be useful in predicting both the projectile-plate interaction and the plate-mechanism interaction. In order to use lumped-parameter methods to simulate the projectile-plate interaction of a ballistic impact onto a fixed armor plate, a model similar to the one shown in Figure 8.4 is required.
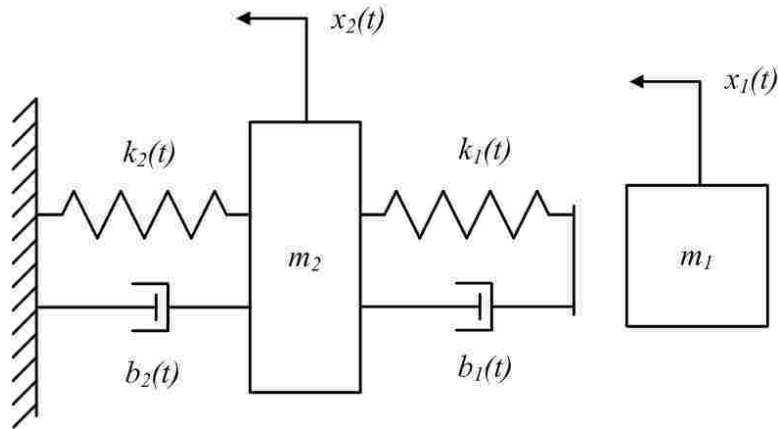
Figure 8.4: Simple ballistic impact lumped-parameter model

Here, the masses of the projectile and the armor plate are represented by the point masses m_1 and m_2, respectively. The elastic energy storage and plastic energy dissipation that occur during the projectile-plate interaction are represented by the springs, k_1 and k_2, and dampers, b_1 and b_2. The two sets of springs and dampers represent two different portions of the impact. The impact occurs as mass m_1 is given an initial velocity causing a collision with the spring k_1 and damper b_1. The system is then allowed to experience its natural vibration behavior. Specific characteristic values are required for each of the system components in order to simulate the projectile-plate interaction.

Unfortunately, values for these parameters are highly nonlinear and difficult to determine. Because of the challenges involved with properly instrumenting ballistic experiments, the literature contains very little progress in the identification of these parameters for a variety of impacts.

In one example, Wu [22] presents a lumped-parameter model intended to simulate low-velocity impacts onto a rigidly-fixed plate. Wu used the same lumped-parameter design as shown in Figure 8.4 but removed the dampers, instead using nonlinear piecewise spring functions for k_1 and k_2 to account for energy dissipation. His modified lumped-parameter model is shown in Figure 8.5. The non-linear springs also have different responses during the loading and unloading, creating hysteresis and energy loss during deflection. The force-deflection relationships are shown in Figures 8.6 and 8.7.
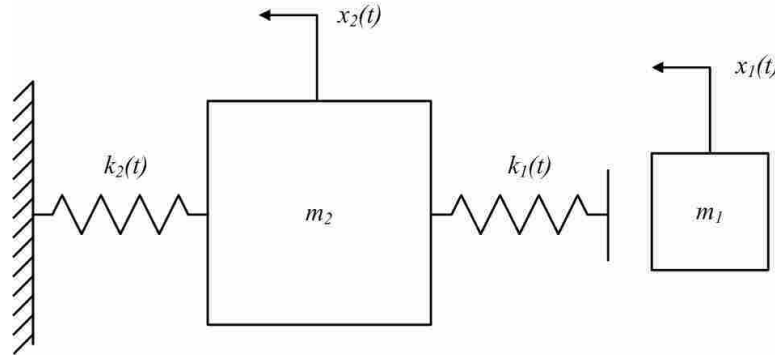
Figure 8.5: Lumped-parameter model used by Wu [22]
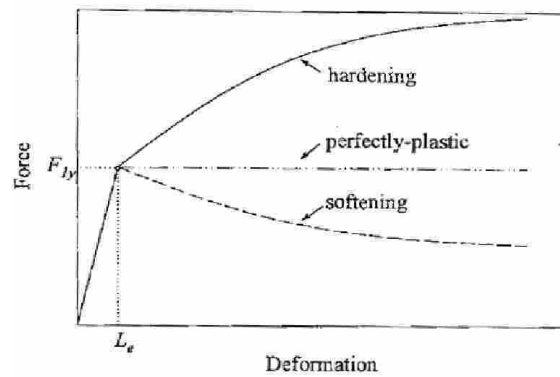
Figure 8.6: Force-deflection relationship for k_2 from Wu [22]

Wu's approach showed some success in predicting certain types of low-velocity ($<$50 m/s) impacts, but no discussion is presented on the required modification of the model parameters for higher velocity ballistic impacts. For these reasons, the lumped-parameter approach is difficult to apply to the projectile-plate interaction in a preliminary study.

The lumped-parameter approach, as mentioned earlier, is also well-suited to simulate the plate-mechanism interaction. A CMRA element's stiffness and damping properties could be measured easily, and used as inputs to the simple model shown in Figure 8.3. Such a model could then receive displacement or force inputs and respond accordingly. Combining the models for the projectile-plate interaction and the plate-mechanism reaction results in the lumped-parameter model shown in Figure 8.4

58
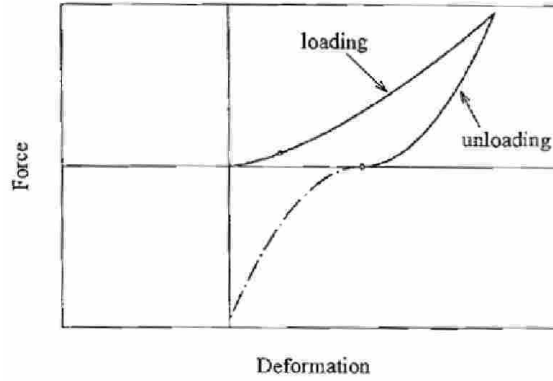
Figure 8.7: Force-deflection relationship for k_1 from Wu [22]
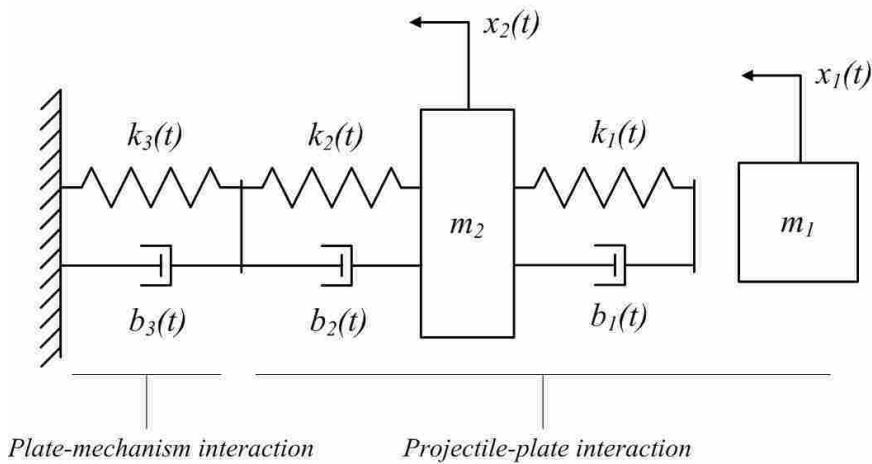
Figure 8.8: Combined lumped-parameter model of projectile-plate and plate-mechanism reaction

8.2.3 Force History Model

Because the projectile-plate interaction presents significant challenges to lumped-parameter modeling, other analytical approaches must be considered for this interaction. Two different analytical models are presented for determination of the contact force during impact.

Modified Fluid Dynamics (Virostek)

As part of their effort to develop new ballistic impact instrumentation methods, Virostek, et al., developed an analytical model capable of predicting the contact force between a

hemispherically-tipped projectile (see Figure 8.9) and metallic armor plate during impact as a function of time [23].

Figure 8.9: Hemispherically-tipped projectile used by Virostek

Rather than requiring an input impact duration to solve for a contact force history, this model uses a modified version of the fluid dynamics drag equation, as shown in Equation 8.4.

$$F(t) = A(t) \left(S_y + \frac{1}{2} C_d \rho v(t)^2 \right) \tag{8.4}$$

where

- $F(t)$ is the contact force at any time t during the impact

- $A(t)$ is the projected area of projectile tip in contact with the target at any time t during the impact

- S_y is the dynamic yield strength of the target

- C_d is the drag coefficient in the target (assumed to be 0.5 by Virostek)

- ρ is the target density

- $v(t)$ is the relative velocity between the projectile and plate at any time t during the impact

The force histories produced by Virostek's modified fluid dynamics model can take various forms, dependent on the input parameters and on whether or not the projectile perforates the plate.

Linearized (Abatan and Hu)

Abatan and Hu [24] present a linearized model capable of simplifying the complex projectile-plate interaction. By applying Newton's second law, the impact force $F(t)$ between a projectile with mass m and velocity v and a fixed plate is determined to be

$$F(t) = m\frac{dv}{dt} \tag{8.5}$$

Assuming that the projectile decelerates to a complete stop upon impact and integrating Equation 8.5, we have

$$\int_0^{t_d} F(t)dt = mV_0 \tag{8.6}$$

where t_d is the impact duration and V_0 is the initial velocity of the projectile. It can be shown from the literature [23] that the force-time relationship ("force history") during projectile impact into plates is roughly a half sinusoid, as seen in Figure 8.10. Imposing this half sinusoid shape, the equation of the force history becomes

$$F(t) = A\sin\frac{t\pi}{t_d} \tag{8.7}$$

where A is the amplitude of the sine wave and the peak impact force. Substituting Equation 8.7 into Equation 8.6 yields

$$A = \frac{mV_0\pi}{2t_d} \tag{8.8}$$
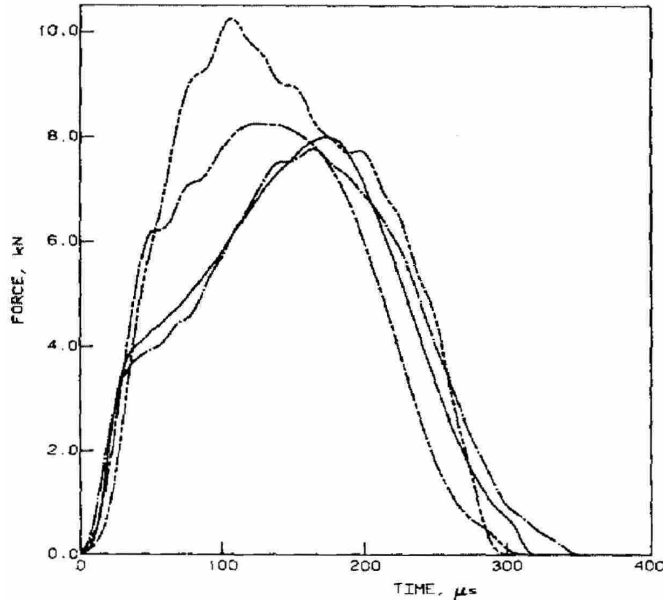
Figure 8.10: Force history plot from Virostek, et al.[23], showing several impact force histories at various impact obliquities

Combining Equations 8.8 and 8.7 results in the final force history relationship, shown in Equation 8.9 and in Figure 8.11, below.

$$F(t) = \frac{mV_0\pi}{2t_d} \sin\frac{t\pi}{t_d} \qquad (8.9)$$

The use of this model for simplification of the projectile-plate interaction requires the choice of an arbitrary impact duration, t_d. If t_d is known for a given impact of this type, this force history relationship will approximate the true impact force history. The selection of the impact duration, then, is the limiting factor in the accuracy of this model.

8.2.4 Initial Velocity Model

The final model to be presented applies to the projectile-plate interaction and is the most simple. In this case, the law of conservation of momentum is again applied to the case of a projectile impact onto a plate at rest. The law of conservation of momentum, as
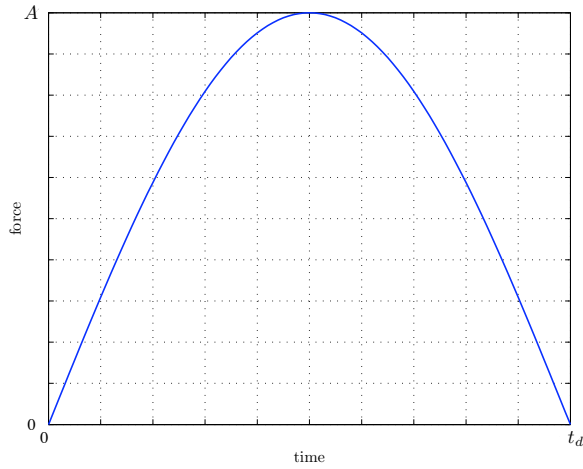
Figure 8.11: Sample force history plot
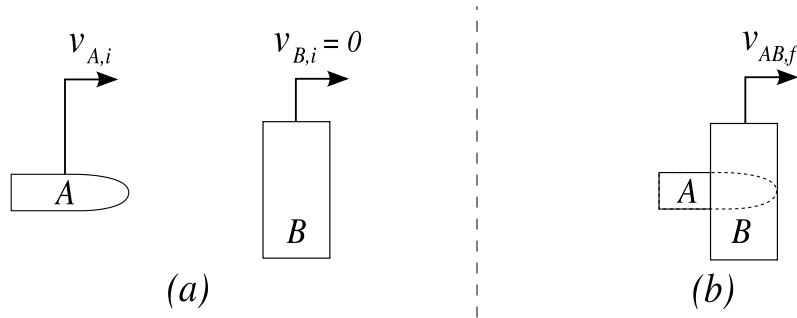
Figure 8.12: Perfectly inelastic collision between a projectile and plate before (a) and after (b) the impact

described earlier, states that momentum is conserved for collisions occurring in the absence of external forces. If a projectile experiences a perfectly inelastic collision with an armor plate, as shown in Figure 8.12, the following momentum balance can be written

$$m_A v_{A,i} = (m_A + m_B) v_{AB,f} \tag{8.10}$$

which can be solved easily for $v_{AB,f}$, as shown in Equation 8.11.

$$v_{AB,f} = \frac{m_A}{m_A + m_B} v_{A,i} \tag{8.11}$$

This final velocity $v_{AB,f}$ can then be used as an input to a lumped-parameter model of the CMRA element to be analyzed. This model ignores all of the complexities of the projectile-plate interaction and assumes that the change in velocity for the plate and projectile at the time of impact occurs instantaneously.

8.2.5 Summary

The strengths and weaknesses of the presented models are summarized in Table 8.1. For the projectile-plate interaction, there are five models available:

- Finite Element

- Lumped Parameter

- Modified Fluid Dynamics Force History

- Linearized Force History

- Initial Velocity

For the plate-mechanism interaction, there are two models available:

- Finite Element

- Lumped Parameter

8.3 Full Evaluation Model

The models described above provide a wide spectrum of options for the desired analysis. Each model is capable of providing some insight into different aspects of a ballistic impact into a CMRA element. The ideal model is simple enough to be both available and useful in the early, repetitive design stage and accurate enough to shed useful insights about the concepts being studied. Models must be selected for both the projectile-plate interaction and the plate-mechanism interaction and then combined into a single analytical model.

64

Table 8.1: Strengths and weaknesses of modeling approaches

Model	Possible Application	Strengths	Weaknesses
Finite Element	Projectile-plate and plate-mechanism	Accurate	Complicated, overly specific
Lumped Parameter	Projectile-plate and plate-mechanism	Simple	Requires unavailable parameters for projectile-plate interaction, assumes non-perforation
Modified Fluid Dynamics Force History	Projectile-plate	Simple	Assumes contact force is modified hydrodynamic drag force
Linearized Force History	Projectile-plate	Simple	Requires choice of impact duration, assumes non-perforation
Initial Velocity	Projectile-plate	Simple	Assumes instantaneous impact, non-perforation

To avoid the inefficiencies and overly specific nature of FE models and the inaccuracies of the initial velocity model, Virostek's modified fluid dynamics force history model is used for the projectile-plate interaction in tandem with lumped-parameter model for the plate-mechanism interaction. These two modeling approaches are combined into one model, as shown in Figure 8.13(a), capable of predicting the dynamic behavior of a CMRA element under impact loading as specified by the forcing history method. The applied force $F(t)$ shown is variable and defined throughout the impact by the forcing history model. Figure 8.13(b) displays the progression of the impact of the bullet into the CMRA element. Note that the center of mass of the plate is accelerated as the plate is penetrated by the bullet.

The programmatical implementation of the evaluation model is shown in Figure 8.14. In the model, the impact is broken up into small time steps, Δt. At the first time step after contact begins, the projectile's initial velocity is used to calculate a depth of penetration, p, into the plate:

$$p = v_{proj}\Delta t \tag{8.12}$$

(a) Full evaluation model schematic   (b) Progression of impact (left to right)
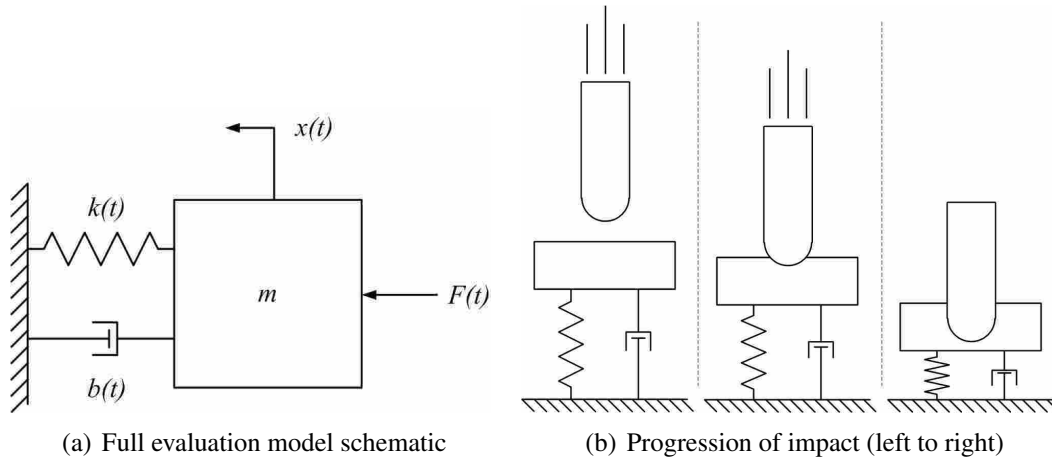
Figure 8.13: Full evaluation model

The contact force is also calculated using the initial projectile velocity for $v(t)$ in Equation 8.4. This contact force, assumed to be constant during the time step, is then used to calculate the decelerated projectile velocity, v_{proj}, at the end of the time step using $F = ma$. The force is also used as an input to the lumped-parameter model of the plate-projectile interaction. This lumped-parameter model is solved for the plate's displacement, d_{plate}, and velocity, v_{plate}, at the end of the time step using a fourth order Runge Kutta ordinary differential equation solver. This plate displacement and velocity are then subtracted from the projectile's depth of penetration and velocity. These reduced values of the depth of penetration and velocity are then used as inputs for the next time step.

This process is then iterated through the duration of the impact until the contact force goes to zero. This occurs when either the projectile comes to equilibrium velocity with the plate, or when the projectile tip completely perforates the rear plane of the plate. Once the force has gone to zero, the lumped-parameter model of the plate-mechanism interaction can be simulated as long as is desired to observe the residual behavior of the CMRA element. Using this approach, the model can predict the total depth of penetration into the armor plate, the maximum deflection of the armor plate, and other responses.

Matlab code for the full evaluation model is contained in Appendix A.

66
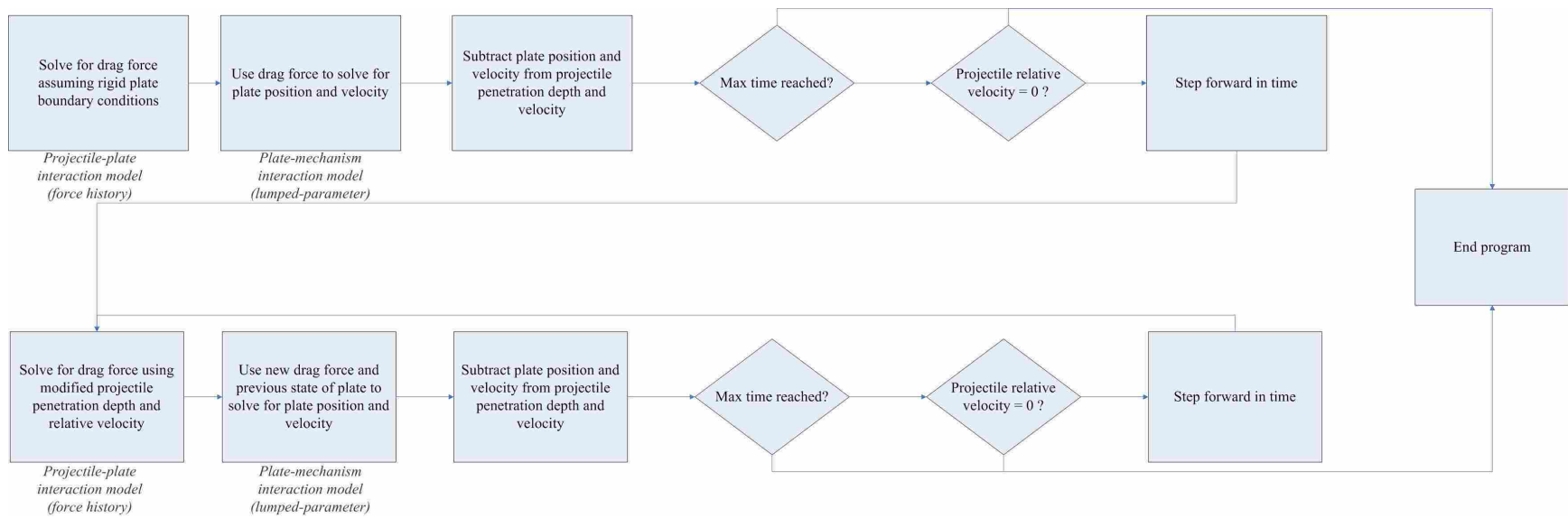
Figure 8.14: Programmatical flowchart of full evaluation model

8.3.1 Full Evaluation Model Assumptions

Projectile-Plate Interaction (Virostek's Force History Model)

There are several assumptions inherent in Virostek's Modified Fluid Dynamics Force History Model. First, the projectile is assumed to be non-deformable and hemispherically-tipped, as shown in Figure 8.9. The target is assumed to exhibit rigid, perfectly-plastic behavior, and to dissipate energy due to dishing or cupping approximately equal to one projectile diameter. The static yield stress is scaled nominally by a factor of 2 due to the side flow resistance presented by the surrounding material [25]. Surface friction has also been ignored in this model because it is assumed to be minimally important [26].

Virostek's model is capable of simulating oblique impacts, but for the initial application of this model for CMRA elements, the impacts are constrained to be normal.

Plate-Mechanism Interaction (Lumped-Parameter Model)

The lumped-parameter model used in modeling the plate-mechanism interaction assumes that the masses, springs, and dampers in the mechanisms can be appropriately approximated by idealized elements. Real springs and dampers are not actually massless and their masses may be significant when compared with CMRA armor plates.

8.3.2 Full Evaluation Model Validation

It is important when introducing new models to perform validation to ensure that the model assumptions do not excessively limit the ability of the model to shed insight into real life phenomena.

Unfortunately, experimental data relevant to modeling this type of impact has not yet been published extensively. One available source of experimental data comes from the photographic impact histories presented by Yang and Xi [27]. Using a high-speed camera, they recorded impacts of projectiles into free-free beams. Projectile impact into a free-free beam, which by definition is subject to no external boundary conditions or forces, is a version of the inelastic collisions discussed in Section 2.3.1. For the region where the inertia of the beam is sufficiently small, the impact results in translational and rotational

acceleration of the beam, as well as the plastic energy dissipation and elastic energy storage which are common to impacts into rigidly fixed structures.

The experimental setup used by Yang and Xi is shown in Figure 8.15. After balancing the target beam vertically on end, they fired projectiles into the beam using a gas gun. A truncated plot of one photo history from their experimentation is shown in Figure 8.16.
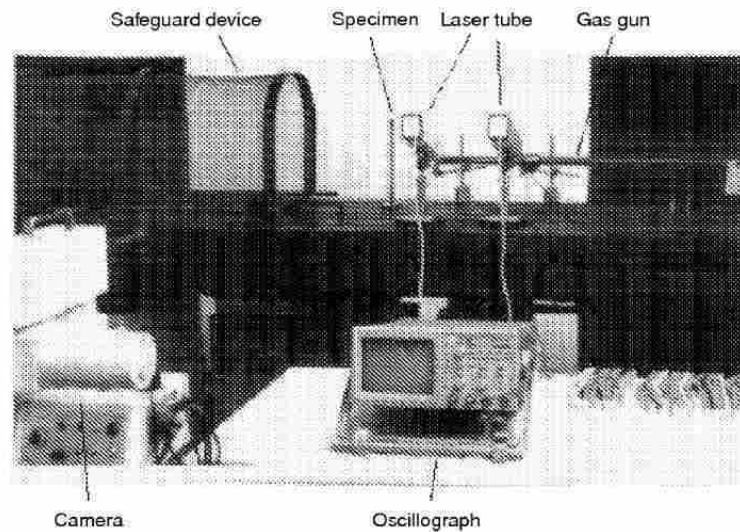
Figure 8.15: Experimental setup used by Yang and Xi [27]

By assuming that the impact duration was completed by the time indicated in the first photograph where the projectile separates from the beam, and by including the same mass and dimensional properties used in the experiment, the proposed final model for CMRA systems can be used to simulate the same experiment. Using the photos from the plot corresponding to the beginning and end of the impact and the known beam dimensions, it is possible to measure the approximate distance traveled by the free-free beam over a given time interval.

As shown in Figure 8.17, the distance traveled by the beam during the first 2.714 ms (when the projectile began to separate from the beam) was approximately 14% of the length of the beam. Because the beam's length was 300 mm, the approximate distance traveled by the beam was 42 mm.
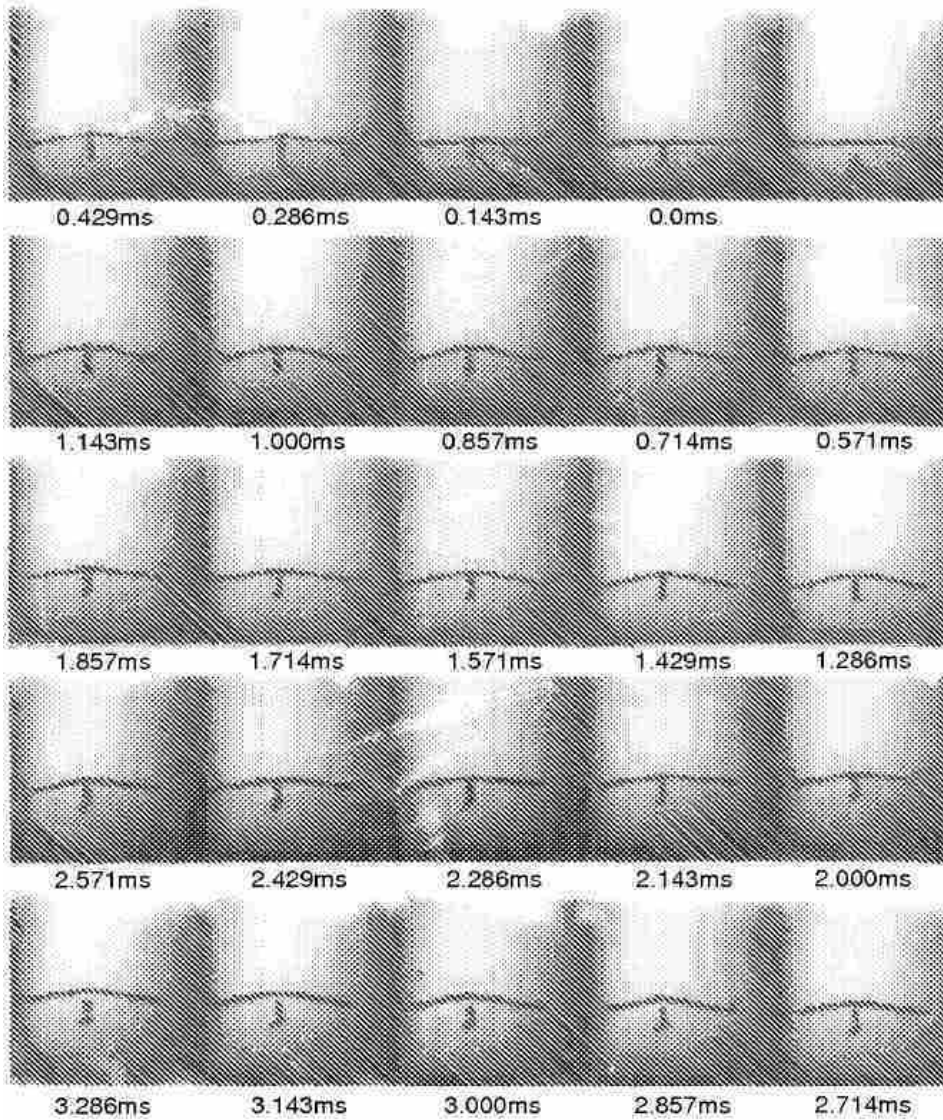
Figure 8.16: Impact photograph history from Yang and Xi [27]

Using the model inputs specified by Yang and Xi and displayed in Table 8.2 and setting the spring and damper coefficients to zero, the dynamic response output of the proposed model was simulated and is shown in Figure 8.18. Because the spring and damper coefficients were set to zero, no force was exerted externally on the plate to resist its motion. Like the free-free beam in Yang and Xi's experiment, the plate would eventually displace indefinitely with constant velocity in the absence of other external forces. The final displacement of the plate at 2.714 ms is seen to be 46.2 mm, which constitutes 10% deviation.

70
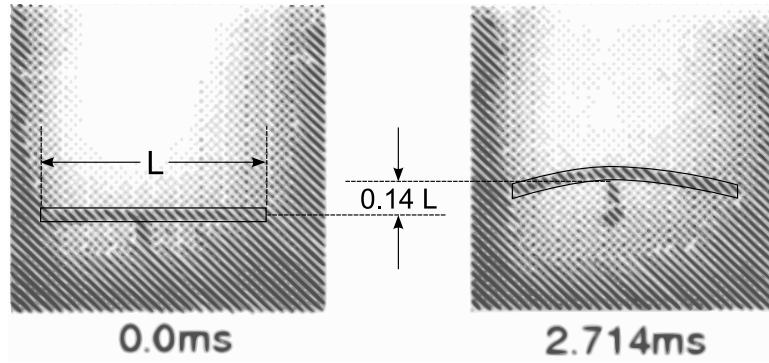
Figure 8.17: Enlarged initial and final photographs from impact photograph history [27]

Table 8.2: Model input parameters as specified by Yang and Xi [27]

Model Input Parameters	Values
m_1 (projectile mass)	0.034 kg
ρ (plate/beam density)	2600 kg/m^3
l_1 (plate/beam base)	0.025 m
l_2 (plate/beam width)	0.01 m
l_3 (plate/beam length)	0.3 m
m_2 (plate/beam mass)	0.195 kg
v_i (projectile initial velocity)	118.2 m/s
t_d (impact duration)	2.714 ms

Even though 10% deviation is likely similar to the resolution of this optical measurement, it does show satisfactory agreement.

8.4 Summary

In order to provide quantitative measures of concept performance, several different modeling options were considered for the two different interactions involved in impact into a CMRA element. One was selected for each of the interactions and the two models were combined into a single full model capable of shedding insights into the behavior of specific CMRA designs.
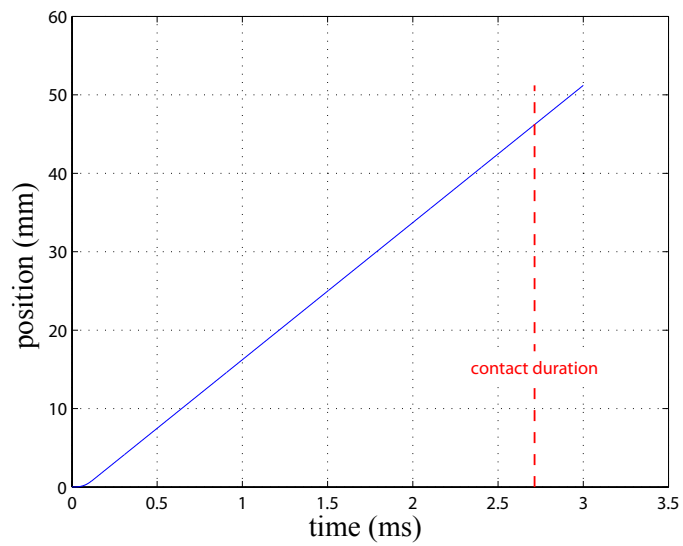
Figure 8.18: Simulated dynamic response of final evaluation model corresponding to experimental results from Yang and Xi

Chapter 9

Design Space Exploration

9.1 Introduction

The selected modeling approach developed in the previous section was used to search the design regions of the selected concepts identified in Chapter 7. The search of the design space is focused on the generalized Spring and Damper concept in order to study the sensitivities of the selected concepts. After completing the search, trends within the design space are identified and discussed. Comparisons to the general case are then provided to evaluate the other concepts. Finally, the desirable regions of the design space are checked for feasibility.

9.2 Model Parameters

In design space search methodology, *analysis variables* are variables used as inputs to the model but are not varied by designers to change the output of the model. These variables can be thought of as constants relevant to the model but not part of the specific individual design. In contrast, *design variables* are variables that designers use to vary the performance of specific designs.

9.2.1 Analysis Variables

The analysis variables in this design space search characterize the specific impact to be examined and the physical constants necessary to the impact simulation. These analysis variables and the values used in the search are displayed in Table 9.1. These values are selected either from the literature [23] or as reasonable starting points for preliminary simulations.

Table 9.1: Analysis variables

Analysis Variable	Definition	Value
$m_{projectile}$	projectile mass	0.0295 kg
R	projectile tip radius	0.00635 m
h	target thickness	0.0254 m
ρ	target density (2024-O Al)	2710 $\frac{\text{kg}}{\text{m}^3}$
S_y	target dynamic strength (2024-O Al)	1.52e7 Pa
C_d	target drag coefficient (2024-O Al)	0.5
v_i	projectile impact velocity	100 $\frac{\text{m}}{\text{s}}$

9.2.2 Design Variables

In this search, there are four primary sets of design variables. These are the impact mass ratio, the plate cocking distance, the damper parameters, and the spring parameters.

Impact Mass Ratio

The impact mass ratio, γ, is defined as the ratio of the mass of the plate to the mass of the projectile:

$$\gamma = \frac{m_{plate}}{m_{projectile}} \tag{9.1}$$

For the characteristic impact used in this search, the projectile weighs 29.5 grams. From preliminary studies, it was determined that the Spring and Damper concept affects the impact significantly when the mass of the armor plate is close to the mass of the projectile. For this reason, the mass ratio is constrained to values between 0.8 and 7.

Cocking Distance

The cocking distance, d, is defined as the distance the armor plate is cocked away from ground in the lumped parameter model, as shown in Figure 9.1. Because the lumped pa-

74

rameter model is defined with positive displacement in the downward direction, this cock-
ing distance is a negative initial displacement. The cocking distance is constrained to be
between 0 and 0.5 m.
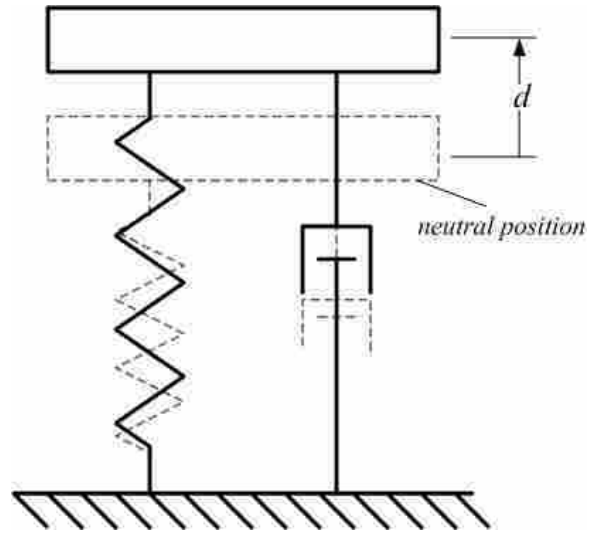
Figure 9.1: Spring and Damper concept with cocking distance, d

Damper Parameters

As explained in Section 8.1.1, the damper included in the Spring and Damper concept is
characterized by two parameters: the damping coefficient, b, and the damping exponent, m.
For this preliminary search, the damper is constrained to linearity by setting $m = 1$. This
results in the simplified relation shown in Equation 9.2. In order to allow the damper the
freedom to approximate some common dampers available in the automotive industry, the
damping coefficient is constrained between 0 and 2000 $\frac{Ns}{m}$.

$$F = b\dot{x} \tag{9.2}$$

Table 9.2: Design variables

Design Variable	Definition	Lower Limit	Upper Limit
γ	mass ratio	0.8	7
d	cocking distance	0 m	0.5 m
b	damping coefficient	$0 \frac{Ns}{m}$	$2000 \frac{Ns}{m}$
k	spring coefficient	$0 \frac{MN}{m}$	$7.5 \frac{MN}{m}$
n	spring exponent	0.1	3

Spring Parameters

As with the damper, the spring included in the Spring and Damper concept is character-ized by two parameters: the spring coefficient, k, and the spring exponent, n, as shown in Equation 9.3. The spring coefficient is allowed to vary between 0 and 10 $\frac{MN}{m}$ to cover an arbitrarily wide range of stiffnesses. The exponent is allowed to vary between 0.1 and 3.0 to permit significant nonlinearity for values of n both above and below 1.

$$F = kx^n \tag{9.3}$$

The constraints imposed upon these design variables during the search are summa-rized in Table 9.2. Some of the plots shown in the following sections may not show the entire possible design space but are zoomed and scaled individually for the best visualiza-tion of the trends within the design space.

9.3 Sensitivity Analyses

The search of the design space for the Spring and Damper concept consists primar-ily of sensitivity analyses, which compare the system performance with various values of the design variables.

The quantitative system performance as simulated by the model developed in Chap-ter 8 is measured primarily as the penetration distance into the plate. The armor plate used

in the model is sufficiently thick to stop the projectile even when rigidly fixed to avoid the extra complication of projectile perforation. Thus, the maximum projectile penetration occurs when the plate's boundary conditions are effectively rigid. The CMRA element is therefore assumed to have no effect on the impact if the penetration does not decrease below that maximum case. Less penetration distance, then, represents a more optimal impact performance because this implies that the CMRA element successfully reduced the severity of the impact. In the following plots, the penetration distance is quantified as a "percent of baseline penetration" which is the ratio of the predicted penetration over the maximum penetration of the rigid boundary condition case. Using the analysis variables specified earlier, the predicted maximum penetration with rigid boundary conditions is 7.129 mm.

A secondary measure of system performance is the maximum distance traveled by the armor plate during the impact. The linear motion undergone by the armor plate during the impact is resisted and ultimately stopped by the spring and/or damper. In order to reduce the overall required size of the armor system, this maximum distance should be kept below a reasonable limit.

It should be noted that the actual quantitative values of these performance measures are representative of only a single characteristic impact. As such, the real value of the sensitivity analysis lies not in the specific values but in the general trends they reveal in the response surface. Some of the plots to be shown below contain some complications beyond the scope of this sensitivity analysis, but the general relationships of use to armor designers are clear.

The following sections will first detail the sensitivities of the model outputs to individual design variables. Following these two-dimensional explorations, the interactions between the design variables will be examined using three-dimensional response surfaces.

9.3.1 Mass Ratio

The effect of the mass ratio upon the penetration depth can be seen in Figure 9.2(a). The penetration depth is shown to increase as the mass ratio increases, but with a decreasing slope. This shows that for very low mass ratios, the penetration depth can be reduced significantly.

The effect of the mass ratio upon the maximum displacement can be seen in Figure 9.2(b). The maximum displacement decreases with increased mass ratio because the transfer of inertia from the projectile to the armor plate results in a lower velocity, and hence a lower maximum armor plate displacement.

(a) Depth of penetration

(b) Maximum armor plate displacement
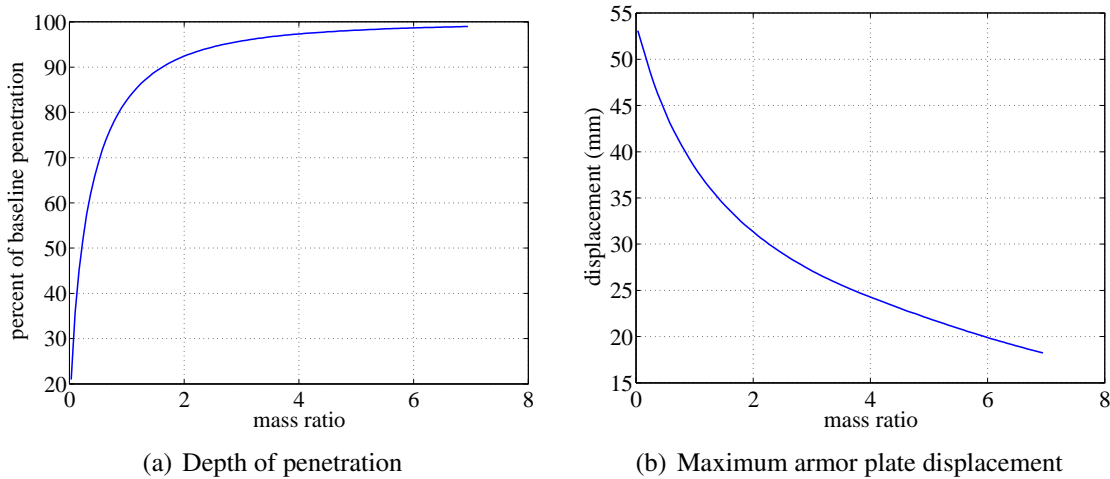
Figure 9.2: Sensitivity plots showing the effect of mass ratio ($k = 100000\frac{N}{m}$, $d = 0$ m, $n = 1$, and $b = 0\frac{Ns}{m}$)

9.3.2   Cocking Distance

The effect of the cocking distance upon the penetration depth can be seen in Figure 9.3(a). The penetration depth is shown to decrease as the cocking distance increases. The inclusion of cocking distance can thus have a significant effect on penetration.

Figure 9.3(b) shows the effect of the cocking distance upon the maximum displacement. The maximum displacement increases with increased cocking distance because there is more kinetic energy in the system once the system reaches the spring's neutral position than there would be without cocking, and the spring requires a greater distance to stop the displacement. The relationship is seen to be nearly linear with a slope of $1 \frac{m}{m}$, which is reasonable because, without damping in the model, the plate should rebound to approximately the same distance with which it was cocked.

These trends serve as motivation for the inclusion of a positive but limited cocking distance in the design. There should be enough cocking to significantly reduce the penetration without significantly increasing the displacement.

(a) Depth of penetration (b) Maximum armor plate displacement
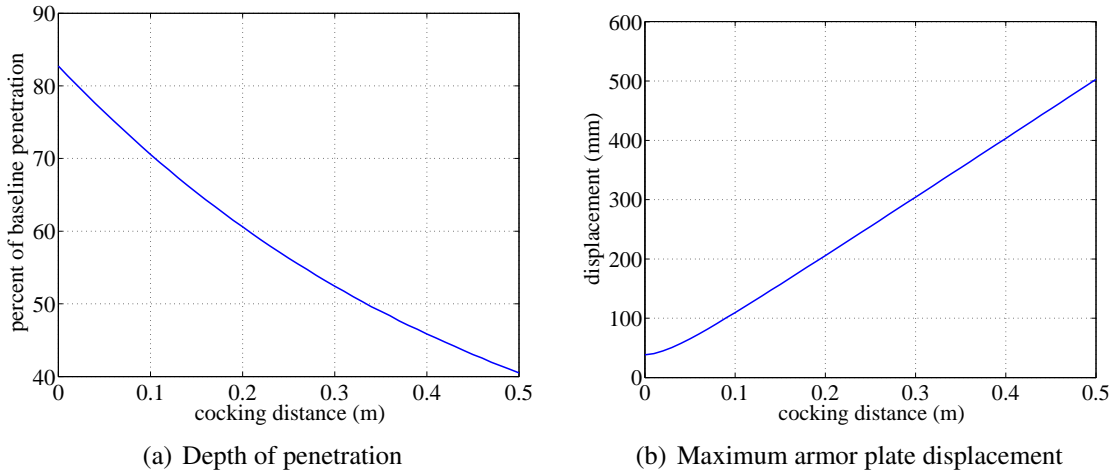
Figure 9.3: Sensitivity plots showing the effect of cocking distance ($k = 100000\frac{N}{m}$, $n = 1$, $\gamma = 1$, and $b = 0\frac{Ns}{m}$)

9.3.3 Damping Coefficient

The effect of the damping coefficient upon the penetration depth can be seen in Figure 9.4(a). The penetration depth increases with the damping coefficient but begins to level off when the damping reaches approximately $1000 \frac{Ns}{m}$.

The effect of the damping coefficient upon the maximum displacement of the armor plate can be seen in Figure 9.4(b). The displacement decreases with increased damping coefficient but begins to level off when the damping reaches approximately $300 \frac{Ns}{m}$.

Even though the damping does decrease the displacement of the armor plate, it clearly has a severely adverse effect on the penetration.

79

(a) Depth of penetration   (b) Maximum armor plate displacement
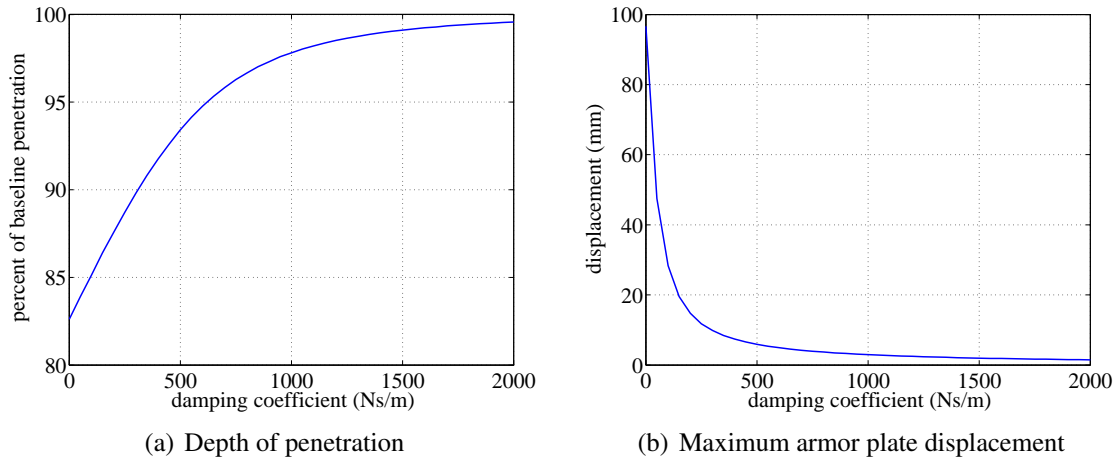
Figure 9.4: Sensitivity plots showing the effect of damping coefficient ($k = 0 \ \frac{\text{N}}{\text{m}}$, $d = 0$ m, $n = 1$, and $\gamma = 1$)

9.3.4   Spring Parameters

Spring Coefficient

The effect of the spring coefficient upon the depth of penetration can be seen in Figure 9.5(a). The spring coefficient is seen to be directly correlated with the depth of penetration. The stiffer the spring is, the greater the magnitude of penetration. This is reasonable because more spring force should correspond to a more rigid boundary condition and greater contact forces and penetrations. The spring coefficient does not, however, increase the penetration as quickly as does the damping coefficient.

The effect of the spring coefficient upon the armor plate displacement can be seen in Figure 9.5(b). Because the displacements of the plate experience greater resistance with greater spring coefficients, the maximum displacements decrease with increased spring coefficients.

As before, the penetration and displacement have competing trends.

Spring Exponent

The effect of the spring exponent upon the plate penetration is shown in Figure 9.6(a). It is interesting to note the abrupt discontinuity in the plot at $n \approx 0.5$. Once the exponent

(a) Depth of penetration　　　　　　(b) Maximum armor plate displacement
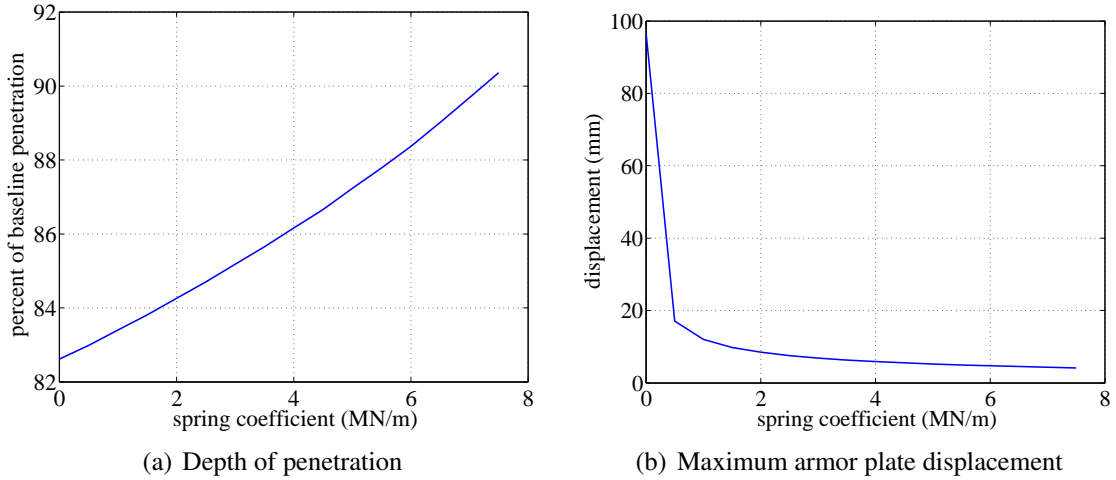
Figure 9.5: Sensitivity plots showing the effect of spring coefficient ($b = 0 \frac{\text{Ns}}{\text{m}}$, $d = 0$ m, $n = 1$, and $\gamma = 1$)

reaches approximately 0.5, the penetration drops significantly. While the exact cause of the discontinuity is unknown, it is reasonable that the initially-steep spring stiffness curve of low exponent springs is much like having a very high spring coefficient, which has been shown to have an adverse effect on plate penetration.

The desirable decrease in penetration above $n \approx 0.5$ begins to level off at $n \approx 1$, with no appreciable effect beyond $n = 1.5$. Unlike the low exponent effect described above, when the exponent exceeds unity and the displacement is less than one unit length, the spring force is very low. This decreased spring force allows the plate to accelerate more quickly and avoid the penetration that would occur with rigid boundary conditions.

The effect of the spring exponent upon the plate displacement is shown in Figure 9.6(b). It is shown that the displacement increases with increased spring exponent. The decreased spring force for these low displacements accounts for the increased displacement for higher exponents.

9.3.5 Interactions

The following sections detail the interactions between the different design variables as they affect the model outputs.

81

(a) Depth of penetration (b) Maximum armor plate displacement
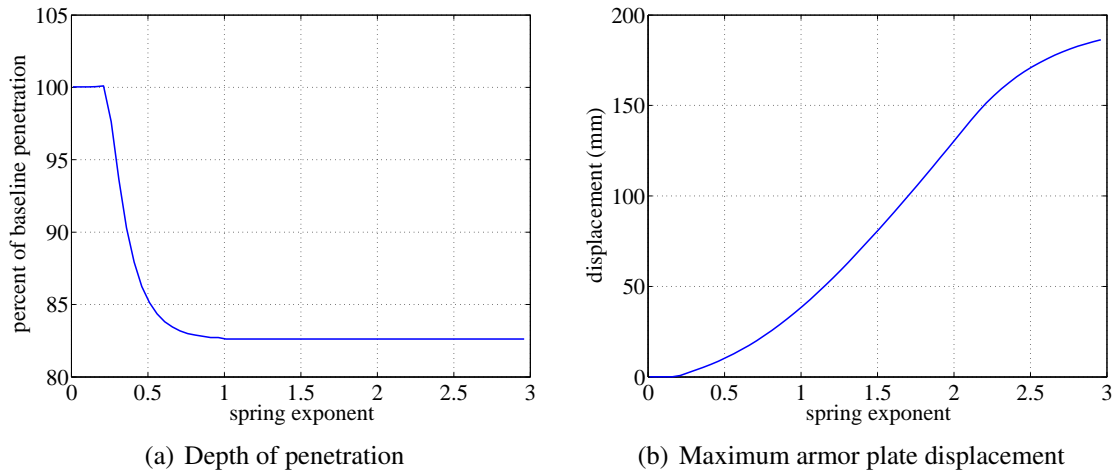
Figure 9.6: Sensitivity plots showing the effect of spring exponent ($b = 0\frac{\text{Ns}}{\text{m}}$, $d = 0$ m, $\gamma = 1$, and $k = 100000\frac{\text{N}}{\text{m}}$)

Mass Ratio and Spring Coefficient

Figure 9.7(a) displays the combined effect of the mass ratio and spring coefficient on the penetration depth plate. This plot is useful for comparing the relative effect of the two design variables on the penetration. It is clear that reducing the mass ratio has a larger effect on the penetration depth than does reducing the spring coefficient.

Figure 9.7(b) displays the effect of the mass ratio and spring coefficient on the maximum plate displacement during impact. Here, the penetration depth has approximately equal sensitivity to changes in the mass ratio and spring coefficient. For low values of spring coefficient, the mass ratio has a significant effect on the displacement. Once the spring coefficient increases significantly, the effect of the mass ratio is diminished. Likewise, the spring coefficient has a greater effect on the displacement for lower values of mass ratio.

Mass Ratio and Spring Exponent

The plot shown in Figure 9.8(a) displays the interaction between the mass ratio and spring exponent as they affect the depth of penetration. This plot illustrates the fact that when the spring exponent is below 0.5, even a low mass ratio does not reduce the penetration depth

(a) Depth of penetration

(b) Maximum armor plate displacement
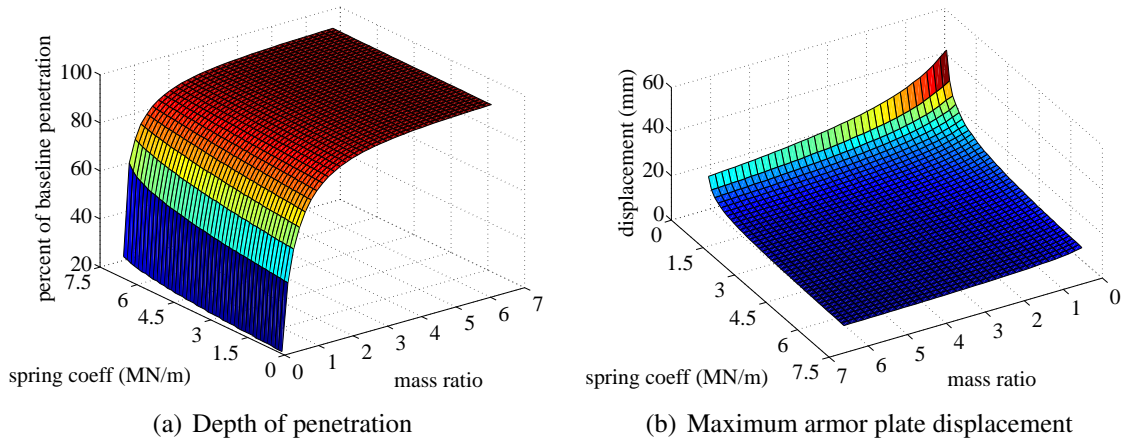
Figure 9.7: Sensitivity plots showing the effect of mass ratio and spring coefficient ($b = 0\frac{\mathrm{Ns}}{\mathrm{m}}$, $d = 0$ m, and $n = 1$)

appreciably. For the region of the plot where $n > 0.5$, it is clear that the the mass ratio has a more profound influence on the penetration depth than does the spring exponent.

Figure 9.8(b) displays the interaction between the mass ratio and spring exponent and their influence on the maximum plate displacement. Increases in the spring exponent increase the maximum plate displacement, as described earlier, and also increase the sensitivity of the displacement to the mass ratio. For larger values of spring exponent more than lower values, increases in the mass ratio produce larger decreases in the maximum plate displacement.

Spring Coefficient and Spring Exponent

Figure 9.9(a) displays the interaction between the spring coefficient and spring exponent and their influence on the depth of penetration. This plot displays a plateau region of penetration for low values of spring exponent corresponding to the peculiarly flat region seen previously at low spring exponents in Figure 9.6(a). This plateau is also seen to grow more and more narrow as the spring coefficient decreases. After bridging that critical edge value of spring exponent, the penetration shows a strong sensitivity to further increases in spring exponent up to approximately $\gamma = 1.5$.

(a) Depth of penetration   (b) Maximum armor plate displacement
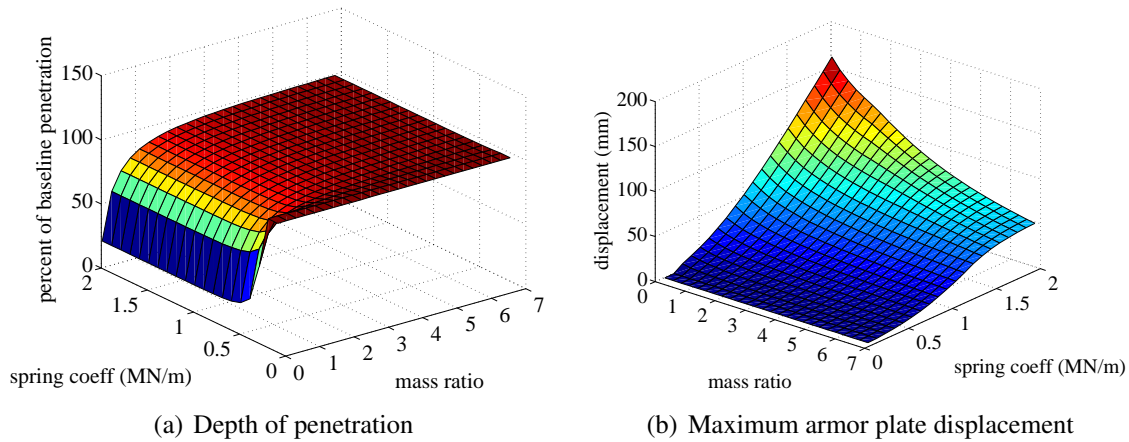
Figure 9.8: Sensitivity plots showing the effect of mass ratio and spring exponent ($b = 0\frac{\text{Ns}}{\text{m}}$, $d = 0$ m, and $k = 100000\frac{\text{N}}{\text{m}}$)

Figure 9.9(b) displays the interaction between the spring coefficient and spring exponent and their influence on the maximum plate displacement. It is clear that for low spring exponents, the displacement shows little sensitivity to the spring coefficient. With increased spring exponent, the spring coefficient begins to affect the displacement more significantly. With lower spring coefficients, the higher spring exponents have a larger positive effect on the maximum displacement. The largest displacements occur when the spring coefficient is low and the spring coefficient is high, both of which result in low spring stiffness for deflections less than 1 m.

Cocking Distance and Mass Ratio

Figure 9.10(a) displays the interaction between the cocking distance and mass ratio and their influence on the depth of penetration. For the entire range of mass ratio, increasing the cocking distance decreases the depth of penetration, although the penetration is more sensitive to cocking distance for lower mass ratios than for larger mass ratios. It is also clear from the figure that, for the range of values examined, penetration depth is generally more sensitive to mass ratio than the cocking distance.

Figure 9.10(b) displays the interaction between the cocking distance and mass ratio and their influence on the maximum plate displacement. The plate displacement's sensi-

(a) Depth of penetration

(b) Maximum armor plate displacement
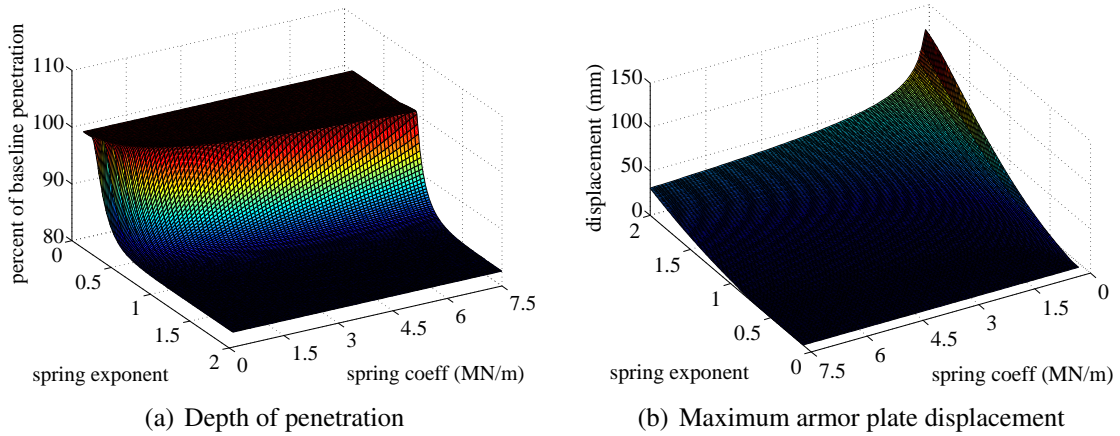
Figure 9.9: Sensitivity plots showing the effect of spring coefficient and exponent ($b = 0\frac{\mathrm{Ns}}{\mathrm{m}}$, $d = 0$ m, and $\gamma = 1$)

tivity to cocking distance is seen to be relatively independent of changes in the mass ratio. The sensitivity to mass ratio is only slightly dependent on the cocking distance, with a diminished sensitivity for higher cocking distances.

It is worthy of noting that for all cases where cocking distance is imposed to the degree studied in this analysis, the maximum plate displacement is calculated to be orders of magnitude greater than otherwise. This is understandable for the reasons regarding the comparability of cocking and displacement mentioned earlier in Section 9.3.2.

(a) Depth of penetration

(b) Maximum armor plate displacement

Figure 9.10: Sensitivity plots showing the effect of cocking distance and mass ratio ($b = 0\frac{\mathrm{Ns}}{\mathrm{m}}$, $k = 100000\frac{\mathrm{N}}{\mathrm{m}}$, and $n = 1$)

Cocking Distance and Spring Coefficient

Figure 9.11(a) displays the interaction between the cocking distance and spring coefficient and their influence on the depth of penetration. For a linear spring and a mass ratio of 1, the cocking distance and spring coefficents have similar effects on the penetration. For low values of spring coefficient, the sensitivity of the penetration depth is to cocking distance is nearly linear but becomes increasingly exponential for increased spring coefficients. This trend ultimately results in a penetration depth which decreases significantly for small, increasing values of cocking distance. Similarly, without any cocking distance, the spring coefficient is not very influential on the penetration depth. With even small increases in cocking distance, however, the model shows significant improvement with increased stiffness.

It is assumed that this is because the increased stiffness, with a positive cocking distance, provides a reverse stiffness to the armor plate complementary to the force applied to the armor plate by the projectile. Thus, the force between the plate and projectile is reduced and the plate and projectile reach equilibrium velocity sooner, resulting in less plate penetration.

Figure 9.11(b) displays the interaction between the cocking distance and spring coefficient and their influence on the maximum plate displacement. This plot shows that the sensitivity of the maximum plate displacement to the cocking distance is fairly independent of the spring coefficient. This is reasonable because, as was stated earlier, the plate should rebound to approximately the same distance with which it was cocked, and this regardless of the stiffness of the spring.

Cocking Distance and Spring Exponent

Figure 9.12(a) displays the interaction between the cocking distance and spring exponent and their influence on the depth of penetration. The same plateau phenomenon in the design space seen in Figure 9.6(a) for low values of spring exponent can again be seen here where there is no cocking distance. As soon as cocking distance is introduced, however, the pen-

(a) Depth of penetration

(b) Maximum armor plate displacement
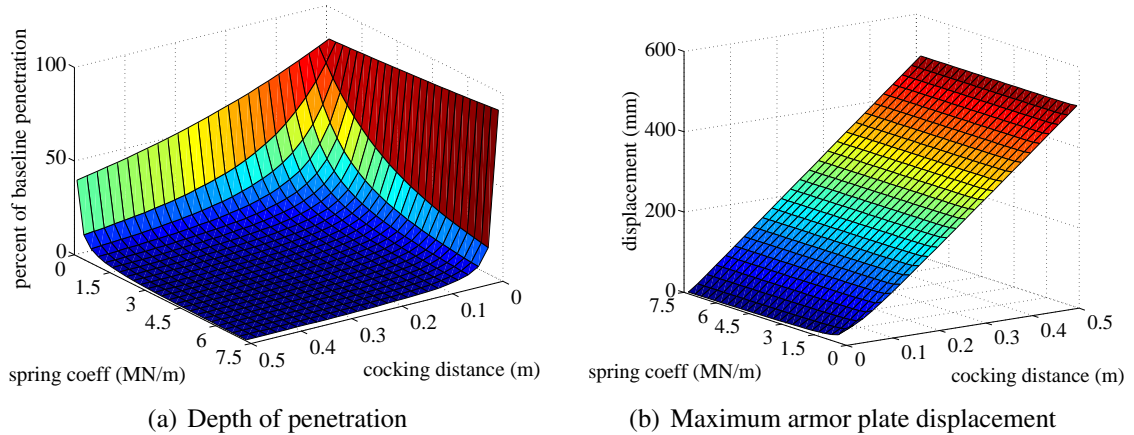
Figure 9.11: Sensitivity plots showing the effect of cocking distance and spring coefficient ($b = 0\frac{\text{Ns}}{\text{m}}$, $n = 1$, and $\gamma = 1$)

etration depth's sensitivity to spring exponent changes dramatically. Here the penetration depth decreases significantly for decreases in spring exponent.

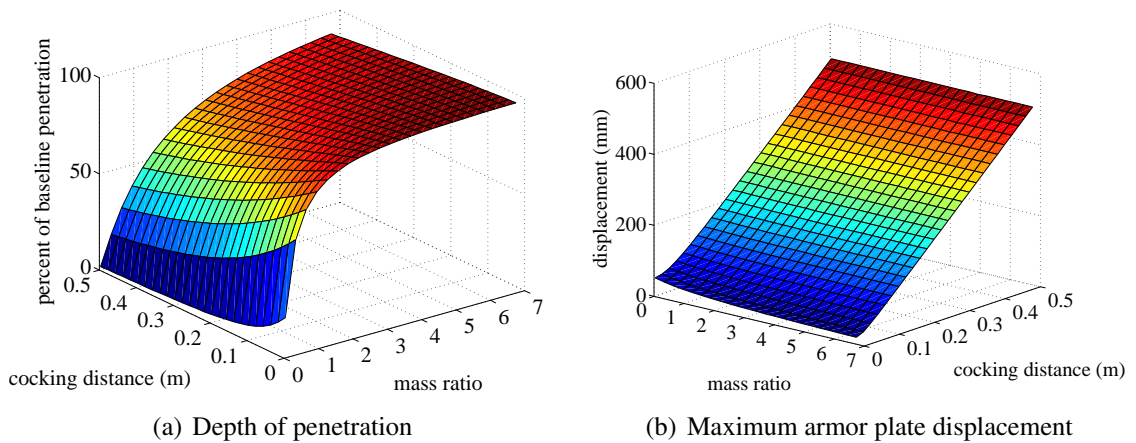Figure 9.12(b) displays the interaction between the cocking distance and spring exponent and their influence on the maximum plate displacement. As seen earlier, the sensitivity of the displacement to the cocking distance is fairly independent of changes in the spring exponent. As the cocking distance increases, the sensitivity of the maximum plate displacement to the spring exponent is diminished.

(a) Depth of penetration

(b) Maximum armor plate displacement
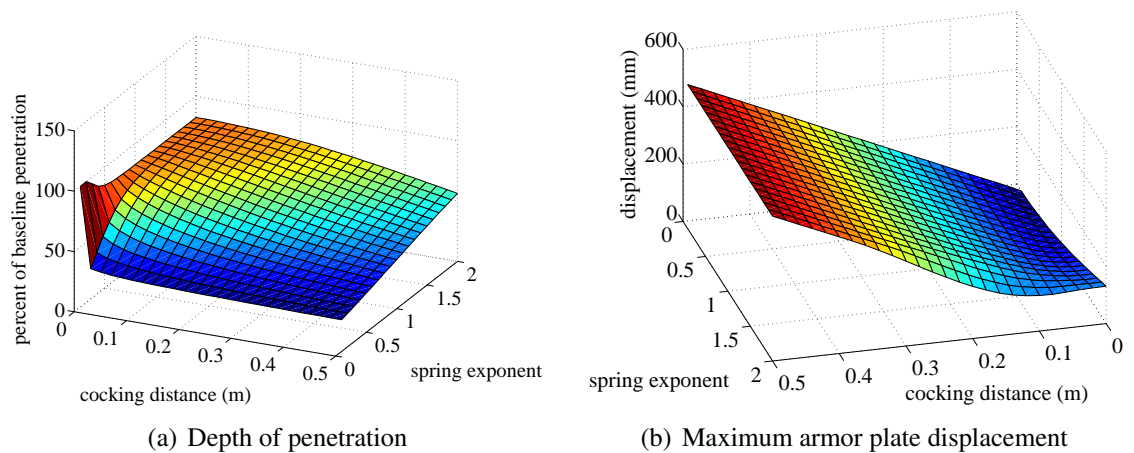
Figure 9.12: Sensitivity plots showing the effect of cocking distance and spring exponent ($b = 0\frac{\text{Ns}}{\text{m}}$, $k = 100000\frac{\text{N}}{\text{m}}$, and $\gamma = 1$)

9.4 Connection to Other Concepts

These sensitivity analyses, as has been explained, were generated specifically for the Spring and Damper model. The Cocked Cantilever and Helical Rotating Spring chosen for further evaluation in Chapter 7 also provide forced resistance to the motion of their respective armor plates during deflection, and their performance can be inferentially considered in light of these sensitivity analyses.

9.4.1 Cocked Cantilever

The Cocked Cantilever mechanism, upon impact and triggered release, would provide a force upon the armor plate mounted at its free end which is complimentary to the contact force from the projectile. Because the plate was initially at rest, it would still accelerate while diminishing the projectile's penetration. The force causing that acceleration would come from the impacting projectile, just as with the Spring and Damper concept, *and* from the cocked cantilever mechanism. After reaching its neutral position, the cantilever would resist and ultimately stop the motion of the plate and embedded projectile, just like the cocked Spring and Damper concept. For these reasons, it is clear that the concept design space of the Cocked Cantilever concept would be similar to that of the Spring and Damper concept.

9.4.2 Helical Rotating Spring

The Helical Rotating Spring mechanism also provides a forcing function to the armor plate during its deflection upon impact. Similar to the Cocked Cantilever, this mechanism could also be cocked and provide the complimentary force to the armor plate upon release at impact. The force-deflection relationships provided by the Helical Rotating Spring and the Cocked Cantilever would have different shapes and thus unique but similar performance. As before, the deceleration of the projectile would not occur until the mechanism had displaced beyond its neutral position. For this reason, it is reasonable to assume that the Helical Rotating Spring would have a similar design space to the cocked Spring and Damper.

9.5 Feasibility Analysis

The feasibility analysis is intended to investigate the practicality of the desirable regions of the design space. The following sections will discuss the feasibility of the general concept and the two selected concepts.

9.5.1 Spring and Damper

The generalized Spring and Damper concept could be practicable if designed simply as a plate with a spring and/or damper mounted on the rear surface. In this case, the concept shows most promise when the mass ratio is very low (at most near unity), when the spring coefficient is low, when the spring exponent is low, when the damping is nonexistent, and when the mechanism is cocked. When cocked, the cocking distance will largely determine the maximum plate displacement (and hence the overall size requirement of the armor system), and must therefore be limited. If the mechanism is not cocked, the spring exponent should be greater than approximately 1.4 or 1.5.

Linear steel compression springs are available within the range of spring coefficients studied in the sensitivity plots, but these grow quite massive ($\gamma > 25$) for the majority of the range. This places the overlap of the desirable and feasible designs in the region where the maximum plate displacement is excessive. One possible method for reducing the overall displacement of the plate would be to use a stop on the plate at some point after the plate and the projectile have reached equilibrium velocity. This would effectively be a highly nonlinear force-deflection curve not well approximated by the low-order polynomials used in this study. After the projectile and plate reach equilibrium velocity, the plate-projectile combination would have velocity below the initial velocity of the projectile and greatly decreased sectional density and could be decelerated simply without large stress concentrations or danger of further penetration.

9.5.2 Cocked Cantilever

Cantilevered beams offer many different force-deflection curves at their free ends. The force-deflection curve depends heavily on the geometry of the beam cross section and the beam's material properties.

From the PRBM method introduced in Section 2.2.1, a cocked cantilever beam can be modeled as two rigid links joined by a pin joint and a torsional spring, as shown in Figure 9.13.

(a) Compliant cantilever beam schematic   (b) PRBM cantilever beam schematic
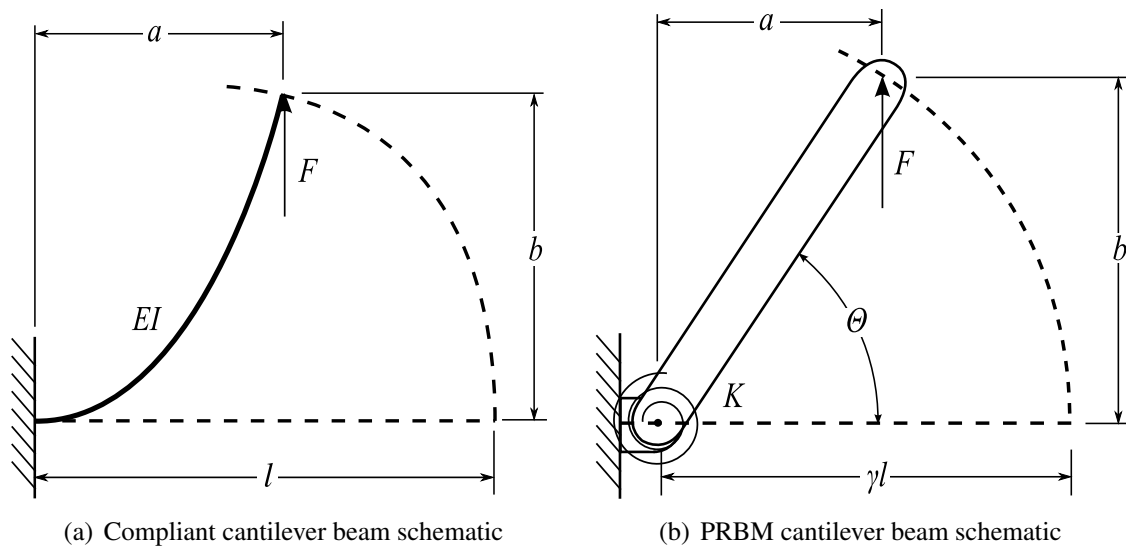
Figure 9.13: PRBM model of Cocked Cantilever concept for feasibility evaluation

Using the material properties of titanium 6-4 for the rectangular beam and other reasonable beam parameters (see Table 9.5.2), the available force at the free tip of the beam was solved for with the PRBM. The force varies with the angle, Θ, or the height of displacement, b, which corresponds to the cocking distance, d. The slope of the force deflection curve, which equates to the effective stiffness in the impact direction, is shown in Figure 9.14(a). Even though the curve shows an increasing stiffness with increasing deflection, the increase in stiffness is minor. Also shown in Figure 9.14 is the stress-deflection relationship along with the yield stress threshold for the titanium.

90

Table 9.3: Beam parameters for Cocked Cantilever feasibility evaluation [5]

Beam Parameter	Value
Modulus of elasticity, E	113.8 GPa
Yield strength, S_y	880 MPa
Width, w	0.03 m
Height, h	0.015 m
Length, l	0.3 m
Characteristic length , γ	0.85
Torsional spring constant, K	7200 $\frac{\text{N}}{\text{rad}}$

From these plots, it can be seen that this specific beam would not be able to provide the more desirable regions of the sensitivity plots shown earlier. The yield stress is reached at $d \approx 0.03$m, where the effective stiffness is only 0.111 $\frac{\text{MN}}{\text{m}}$. From Figure 9.11, even if the mass ratio were kept near unity, it is clear that penetration reduction would be minimal.

In order to make available the more desirable regions of the design space, a number of different designs might be necessary. Improved and possibly variable cross sections and material properties would allow the Cocked Cantilever to achieve greater penetration reduction by allowing increased cocking distance and effective stiffness and decreased mass.

9.5.3 Helical Rotating Spring

The Helical Rotating Spring, because of the number of initially-curved beams supporting the plate, has potential for a great deal of nonlinear cocked stiffness, which would magnify the cocking distance effect relative to the Cocked Cantilever. Unfortunately, very similar stress and geometric constraints apply to this concept as to the Cocked Cantilever, and the same special design considerations would be required to make available the best regions of the design space. In order to make the concept feasible and desirable, the support beams would need to have low mass, high stiffness, and large cocking distances to provide the low impact stiffness shown to be desirable in the sensitivity analyses.

(a) Effective spring coefficient

(b) Maximum stress in beam
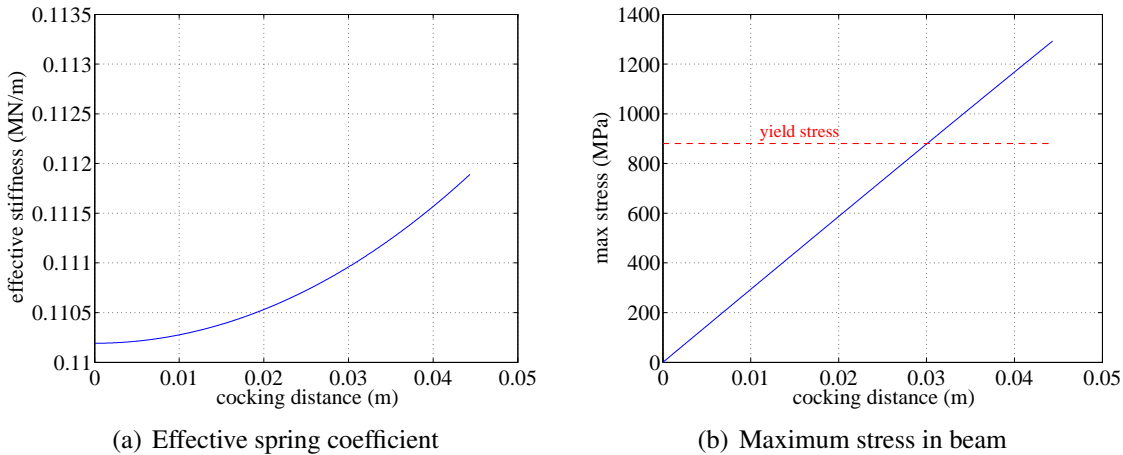
Figure 9.14: Cocked Cantilever effective stiffness and maximum stress

9.6 Summary and Discussion

This section has employed the concept evaluation model developed in Chapter 8 to explore the design space of the Spring and Damper concept. The major trends identified within the design space drive the designer to make the following efforts:

- lower the mass of the armor plate as much as is reasonable

- cock the mechanism as much as is reasonable

- minimize the stiffness of the spring

- as long as the mechanism is cocked, employ a nonlinear spring with a minimal exponent

- eliminate damping from the CMRA element

These same trends apply to the other concepts selected in Chapter 7 inasmuch as they provide forced, unidirectional deceleration to the projectile. The Cocked Cantilever and Helical Rotating Plate both must use these trends to improve their performance in reducing the projectile's penetration depth into the armor plate.

The trend of improved performance with increased cocking distance and reduced stiffness and damping applies exclusively to the impact case where the armor plate deflects

directly backwards in line with the normal impact of a projectile. This improved performance is due to the satisfaction of the controlled stiffness mechanical function discussed in Section 5.1.2.

The satisfaction of this principle, however, is optimal only for reducing penetration for these simple in-line impacts, and does not improve the likelihood of projectile ricochet, yaw, tumble, or break-up. The Spring and Damper mechanism, when designed within the desirable regions identified in this chapter, would reduce penetration only for certain impacts. These or other mechanisms could potentially be designed to satisfy these trends and still provide other mechanical functions to improve the likelihood of projectile defeat.

The brief feasibility analysis was performed to judge the practicality of real-life implementations of these concepts. All three designs appear to be feasible and practicable, although all three would likely be benefited by the use of mechanical stops to increase the nonlinearity of the force deflection.

Chapter 10

Conclusions and Recommendations

This chapter will summarize the accomplishments of this thesis in developing new forms of ballistic armor capable of meeting the advanced requirements of modern armor systems. Conclusions are drawn from the research and modeling efforts and recommendations are provided for future work.

10.1 Conclusions

This thesis has successfully accomplished the research objectives laid out in Chapter 1. The fulfillment of these objectives is outlined in the following major contributions.

10.1.1 Definition of MRA and CMRA

A new field of ballistic armor called Mechanically Reactive Armor (MRA) has been identified and defined as armor which minimizes a kinetic energy projectile's penetration power by using a kinematic mechanism or linkage to effectively deflect or absorb its kinetic energy. Compliant Mechanically Reactive Armor (CMRA) is a subset of MRA where the primary armor mechanism is compliant. CMRA elements are further defined as building blocks of a CMRA system, and may include traditional solid armor plates as well as the primary armor mechanism.

10.1.2 Design Principle Identification

Drawing from the physical relationships controlling ballistic impacts, principles governing the design of Mechanically Reactive Armor have been identified. These principles focus on modifying the parameters of interest in the physical impact phenomena

discussed earlier, and thereby provide a theoretical basis for improved armor performance. The principles are organized into families which have a similar approach.

10.1.3 Mechanical Function Identification

Founded upon the design principles, the mechanical functions required by any successful MRA element are outlined. These mechanical functions are the actual physical behavior of a mechanism required in order to provide the prescribed modification of the significant impact parameters.

10.1.4 Concept Generation

A preliminary set of concepts capable of providing one or more of the requisite mechanical functions has been defined. These concepts effectively populate the design principle families mentioned earlier.

10.1.5 Model Development

A quantitative evaluation model has been developed which is capable of simulating ballistic impact into CMRA concepts. This model provides valuable coupling between the two complicated impact reactions: the projectile-plate interaction and the plate-mechanism interaction.

10.1.6 Design Space Exploration

Using the quantitative evaluation model, the design space of the most general concept was studied. Sensitivity plots shed insight into the trends within the design space and confirm the importance of the design principles identified earlier.

10.2 Recommendations for Future Work

The modeling efforts presented in this thesis correspond primarily to a single representative impact. Greater insight would be gained from exploring a variety of different impacts, including different projectile types and higher velocity impacts.

Other concepts could certainly be developed which may be able to more effectively combine the mechanical functions outlined in this thesis. Such concepts might focus on handling repeat hits, arranging elements into successful arrays, and combining the desirable traits of different concepts into hybrid concepts.

To make further contributions to the development of CMRA systems, it is recommended that improved models for both the projectile-plate interaction and the plate-mechanism interaction be developed. These models would be capable of even greater accuracy in capturing the higher-order vibrations and nonlinear behavior of a CMRA element during impact. The models could also be used to simulate a variety of different impact conditions on the concepts.

Optimization founded upon these higher fidelity models could also be used to isolate the most desirable designs of the most promising concepts. After performing this modeling simulations of the CMRA impacts, experimental data would be very useful for ultimate performance measures. Prototypes of concepts could be instrumented and impacted in such a manner as to further validate the modeling phases of this and future research.

After identifying the most desirable designs from empirical testing, the concepts should be redesigned for manufacturability and mass production.

Appendix A

Matlab Impact Simulation Code

A.1 main_noloop.m

```
% main_noloop.m
%
% Programmed / Edited by Cameron Andersen
%
% June 14, 2007
%
% Matlab script file for simulating ballistic impact into Compliant
% Mechanically Reactive Armor (CMRA) elements.  This simulation effectively
% combines the derivation for contact force during a ballistic impact given
% by Virostek, et al. with a lumped-parameter model of a mass-spring-damper
% dynamic system representing a simplified CMRA element.  The impact
% simulation is based on Virostek's FORTRAN code and the lumped-parameter
% model is based on the solution of a 4th order Runge Kutta differential
% equation solver.
%

% ---------------------------------------------------------

tic                              % start timer
clear                            % clear variables from previous run
format compact                   % compact output
disp('Program running...')

% ------------ Projectile Parameter Initialization
%
% The projectile is assumed to be a hemispherically-tipped cylindrical
% projectile.  These parameters are given in Virostek's paper.
%

m1 = 0.0295;                     % projectile mass (kg)
R = 0.00635;                     % projectile tip radius (m)

% ------------ Plate Parameter Initialization
%
% The armor plate is the link between the ballistic impact and the
% spring-damper system representing the CMRA element.  The values given
% here are specific to a 2024 Aluminum plate.  The dynamic stress factor
% and the drag coefficients are specified in Virostek's paper.
%

h = 0.0254;                      % plate thickness (m)
rho = 2780;                      % plate density (kg/m^3)
m2 = 0.1;                        % mass of plate (kg)
Sy = 75.8e6;                     % static yield strength (Pa)
dyn = 2;                         % static to dynamic stress factor
Syd = Sy * dyn;                  % flow strength (Pa)
Cd = 0.5;                        % drag coefficient

% ------------ Impact Parameter Initialization

y = [0,0];                       % CMRA plate initial pos (m), vel (m/s)
theta = 0/180*pi;                % angle of incidence (rad)
vi = 100;                        % initial projectile velocity (m/s)

% ------------ CMRA parameters

b = 0;                           % damping coefficent (Ns/m)
m = 3;                           % damping exponent
k = 0;                           % spring coefficient (N/m)
n = 3;                           % spring exponent

% ------------ Simulation Parameter Initialization

t = 0;                           % initial time (s)
tmax = 0.0002;                   % stop time (s)
dt = 0.000001;                   % time step (s)
i = 0;
```

```
% ------------ Preprocessing and Simulation Variable Definitions
%
% A = projected area of projectile tip which is in contact with the target
% for any given depth of penetration (m^2)
% Ain = projected area for frontal plane of target plate only (m^2)
% Aout = projected area for distal plane of target plate only (m^2)
% F = resultant force exerted between plate and projectile for any given
% depth of penetration (N)
% Fi = calculated force from previous time step (N)
% p = penetration of projectile nose into front plane of plate (m)
% po = penetration of projectile nose into rear plane of plate (m)
% Pen = total abs. disp. of projectile during impact (m)
% Pt = effective plate thickness (m)
% pF = maximum contact force reached during impact (N)
% v = projectile velocity at any time step (m/s)
% vrel = relative velocity between projectile and plate, used in force
% calculation (m/s)
% pplate = position of plate (m)
% vplate = velocity of plate (m/s)
% output1 = matrix storing projectile behavior; [t, v, Pen, F, A, p]
% output2 = matrix storing plate behavior; [pplate, vplate]

v = vi;
vrel = vi;
Pen = 0;
Fi = 0;
A = 0;
output1 = [t,v,Pen,Fi,A,0];
output2 = [y];
pF = 0;
Pt = h/cos(theta);
mv = m1*vi;

% ------------ Loop

while i >= 0,
    m50
    m200
    m300
end


% ------------ Extract Results from Matrices

t1 = output1(:,1);
impdur = t1(end)*1000              % multiply by 1000 for ms
ttot = [output1(:,1);thist];       % concatenate time from two matrices
vel = output1(:,2);
Pen = output1(:,3)*1000;           % multiply by 1000 for mm
F = output1(:,4);
A = output1(:,5);
p = output1(:,6)*1000;             % multiply by 1000 for mm
pplate = [0;output2(:,1)*1000];    % multiply by 1000 for mm
vplate = [0;output2(:,2)];


% ------------ Plot Results

caseid = 1;

switch caseid
    case 1
        figure(1); clf;
        subplot(221)
        plot(t1,Pen,ttot,pplate,':')
        xlabel('time (s)');
        ylabel('position (mm)');
        title('Absolute Position of Projectile and CMRA Plate');
        grid;
        xl = xlim;

        subplot(222)
        plot(t1,vel,ttot,vplate,':')
        xlabel('time (s)');
        ylabel('velocity (m/s)');
        title('Velocity of Projectile and CMRA Plate');
        grid;

        subplot(223)
        plot(t1,F);
        xlabel('time (s)');
        ylabel('force (N)');
        title('Contact Force During Impact');
        grid;
        xlim(xl)

        subplot(224)
        plot(t1,p,0,0,':');
        xlabel('time (s)');
        ylabel('depth of penetration (mm)');
        title('Depth of Penetration');
        legend('Projectile','CMRA Plate','Location','SouthEast')
```

```
            grid;
            xlim(xl)

end

% ------------ Print Key Results

PeakForce = pF/1000              % peak impact force (kN)
MaxPen = max(p)                  % max penetration depth into plate (mm)
MaxDisp = max(pplate)            % max plate displacement (mm)
elapsed = toc;                   % stop timer
```

A.2 m50.m

```
% m50.m

ti = i * dt;
if i > 0
    if vrel(end) < 0.01 | A == 0,
        [output2,thist] = simulator(ti,y,dt,tmax,m2,b,m,k,n,m1,output2);
        break;
    end
end

Pen = Pen + v*dt;
if i>0,
    p = Pen*Pt/(Pt + 2*R) - real(output2(end,1)-output2(end-1,1));
else
    p = Pen*Pt/(Pt + 2*R);
end



if Pen > (Pt + 2*R)
    p = Pen - 2*R - real(output2(end,1)-output2(end-1,1));
end
if p < 0,
    break
end

% determine the projected normal area of the tip as it penetrates the
% frontal area of the plate

if p >= R*(1/cos(theta)+tan(theta)),
    Ain = pi*R^2;
    m200
end
Ain = pi*(cos(theta))^2*p*(2*R-p*cos(theta));
if theta == 0;
    m200
end
if p > R * (1/cos(theta)-tan(theta))
    z = p/tan(theta)-R*(1/sin(theta)-1);
    s = sin(theta-asin((R-p*cos(theta))*sin(pi-theta)/R/sin(theta)))*R/sin(pi-theta);
    Re = (p*cos(theta)*(2*R-p*cos(theta)))^0.5;
    A1 = (Re^2*acos((Re-s)/Re)-(Re-s)*(s*(2*Re-s))^.5)*cos(theta);
    A2 = (R^2*acos((R-z)/R)-(R-z)*(z*(2*R-z))^.5);
    Ain = Ain - A1 + A2;
end
```

A.3 m200.m

```
% m200.m

po = p - h/cos(theta);
Aout = 0;
if po >= R*(1/cos(theta)+tan(theta)),
    Aout = pi*R^2;
    % jump to 300
    m300
end
if po > 0
    Aout = pi*(cos(theta))^2*po*(2*R-po*cos(theta));
end
if theta == 0
    % jump to 300
    m300
end

if po > R*(1/cos(theta)-tan(theta)),
    z = po/tan(theta) - R*(1/sin(theta)-1);
    s = sin(theta-asin((R-po*cos(theta))*sin(pi-theta)/R/sin(theta)))*R/sin(pi-theta);
    Re = (po*cos(theta)*(2*R-po*cos(theta)))^.5;
    A1 = (Re^2*acos((Re-s)/Re)-(Re-s)*(s*(2*Re-s))^.5)*cos(theta);
    A2 = (R^2*acos((R-z)/R)-(R-z)*(z*(2*R-z))^.5);
    Aout = Aout-A1+A2;
end
```

A.4   m300.m

```
A = Ain - Aout;


% calculate the resultant predicted force on projectile and use the impulse
% to find the new velocity

F = A*(Cd*0.5*rho*vrel^2+Syd);
v = v-dt*(F+Fi)/2/m1;
if F > pF,
    pF = F;
end
Fi = F;

% write output for projectile's history
output1 = [output1;ti,v,Pen,F,A,p];

% call simulation to find next values of plate position and velocity
y = [output2(end,1),output2(end,2)];
output2 = [output2;runge4(ti,y,dt,m2,b,m,k,n,m1,F)];

i = i + 1;

vrel = v - output2(end,2);

% if F == 0 & i ~= 0,
%     break
% end

continue
```

A.5   simulator.m

```
% simulator.m

function [output2,thist] = simulator(t,y,dt,tmax,m2,b,m,k,n,m1,output2);

thist = t;

while(t<tmax),

    y = runge4b(t,y,dt,m2,b,m,k,n,m1);

    t = t + dt;

    output2 = [output2;y];        % augments the results matrix with the new values

    thist = [thist;t];

end
```

A.6   runge4b.m

```
% runge4b.m

function y = runge4b(t,x,dt,m2,b,m,k,n,m1);

ka1 = dt * state2(t,x,m2,b,m,k,n,m1);
ka2 = dt * state2(t + dt/2, x + ka1/2,m2,b,m,k,n,m1);
ka3 = dt * state2(t + dt/2, x + ka2/2,m2,b,m,k,n,m1);
ka4 = dt * state2(t + dt, x + ka3,m2,b,m,k,n,m1);
rk = (ka1 + ka4)/6 + (ka2 + ka3)/3;
y = x + rk;
```

A.7   state2.m

```
% state2.m

function xdot = state2(t,x,m2,b,m,k,n,m1)

xdot = zeros(2,1);
xdot(1) = x(2);
xdot(2) = 1/(m2+m1)*(- b*(abs(x(2)))^m - sign(x(1))*k*(abs(x(1)))^n);
xdot = xdot';
```

A.8   runge4.m

```
% runge4.m

function y = runge4(t,x,dt,m2,b,m,k,n,m1,F);

ka1 = dt * state(t,x,m2,b,m,k,n,m1,F);
ka2 = dt * state(t + dt/2, x + ka1/2,m2,b,m,k,n,m1,F);
ka3 = dt * state(t + dt/2, x + ka2/2,m2,b,m,k,n,m1,F);
ka4 = dt * state(t + dt, x + ka3,m2,b,m,k,n,m1,F);
rk = (ka1 + ka4)/6 + (ka2 + ka3)/3;
y = x + rk;
```

A.9   state.m

```
% state.m

function xdot = state(t,x,m2,b,m,k,n,m1,F)

xdot = zeros(2,1);
xdot(1) = x(2);
xdot(2) = 1/m2*(F - b*(abs(x(2)))^m - sign(x(1))*k*(abs(x(1)))^n);
xdot = xdot';
```

Bibliography

[1] T. Eshel, "Up-armored humvee," *Defense Update*, vol. 3, 2004. [Online]. Available: http://www.defense-update.com/features/du-3-04/up-armored-humvee.htm

[2] M. Liu, J. Barry, and M. Hirsh, "The human cost," *Newsweek*, vol. May 3, 2006. [Online]. Available: http://www.msnbc.msn.com/id/4825948/site/newsweek/

[3] A. Harrison and N. Jones, Eds., *Materials and Structures for Energy Absorption*. Professional Engineering Publishing, Ltd., 2000.

[4] R. C. Laible, Ed., *Ballistic Materials and Penetration Mechanics*. Elsevier Scientific Publishing, 1980.

[5] L. L. Howell, *Compliant Mechanisms*. New York: John Wiley & Sons, 2001.

[6] T. W. Ipson, R. F. Recht, and W. A. Schmeling, Naval Weapons Center, 1973, NWC TP5607.

[7] T. W. Ipson and R. F. Recht, "Ballistic-penetration resistance and its measurement," *Experimental Mechanics*, vol. 15, p. 249, 1975.

[8] M. E. Backman and S. A. Finnegan, Naval Weapons Center, 1976, NWC TP5844 (AD A030268).

[9] G. H. Daneshi and W. Johnson, "The trajectory of a projectile when fired parallel and near to the free surface of a plastic solid," *INT J MECH SCI*, vol. 20, p. 255, 1978.

[10] H. F. S. L. B. G. Jonas A. Zukas, Theodore Nicholas and D. R. Curran, *Impact Dynamics*. Wiley-Interscience, 1982.

[11] A. Tate, "A simple estimate of the minimum target obliquity required for the ricochet of a high speed long rod projectile," *J PHYS D APPL PHYS*, vol. 12, pp. 1825–1829, 1979.

[12] ——, "A theory for the deceleration of long rods after impact," *Journal of the Mechanics and Physics of Solids*, vol. 15, p. 387, 1967.

[13] R. Zaera and V. Sanchez-Galvez, "Analytical modeling of normal and oblique ballistic impact on ceramic/metal lightweight armours," *INT J IMPACT ENG*, vol. 21, no. 3, pp. 133–148, 1998.

[14] G. W. Stone, "Projectile penetration into representative targets," Sandia National Laboratory, October 1994, SAND94-1490, UC-704.

[15] "FAS Military Analysis Network," May 2007. [Online]. Available: http://www.fas.org/man/dod-101/sys/land/m993.htm

[16] M. Macaulay, *Introduction to Impact Engineering*. J. W. Arrowsmith, Ltd., 1987.

[17] N. Shactman, "U.S. military uses the force," Wired Magazine, August 2002. [Online]. Available: http://www.wired.com/science/discoveries/news/2002/08/54641?currentPage=all

[18] A. Mead and S. Ellison, "New age electric armour tough enough to face modern threats," Defense Science and Technologies Laboratory (UK), July 2002. [Online]. Available: http://www.dstl.gov.uk/news_events/press/pr2002/01-07-02.php

[19] W. F. Donovan, "Armor for defeating kinetic energy projectiles," US Patent 5402704, April 1995.

[20] D. L. O. G. R. J. Charles E. Anderson, Jr., "Multi-layered trap ballistic armor," US Patent 7077048, July 2006.

[21] K. Ulrich and S. Eppinger, *Product design and development*. McGraw-Hill New York, 1995.

[22] K. Q. Wu and T. X. Yu, "Simple dynamic models of elastic-plastic structures under impact," *INT J IMPACT ENG*, vol. 25, pp. 735–754, 2001.

[23] S. P. Virostek, J. Dual, and W. Goldsmith, "Direct force measurement in normal and oblique impact of plates by projectiles," *INT J IMPACT ENG*, vol. 6, pp. 247–269, 1987.

[24] A. Abatan and H. Hu, "Effect of cross section material distribution on impact response of hybrid composites," *Journal of Thermoplastic Composite Materials*, vol. 15, pp. 375–387, 2002.

[25] F. E. H. J. Liss, W. Goldsmith, "Constraint to side flow in plates," *Journal of Applied Mechanics, Transactions of ASME*, vol. E50, pp. 694–698, 1983.

[26] J. M. Krafft, "Surface friction in ballistic penetration," *Journal of Applied Physics*, vol. 26, pp. 1248–1253, 1955.

[27] J. L. Yang and F. Xi, "Experimental and theoretical study of free-free beam subjected to impact at any cross-section along its span," *INT J IMPACT ENG*, vol. 28, pp. 761–781, 2003.